Motion of particles and photons in the gravitational field of a rotating body (In memory of Vladimir Afanas'evich Ruban)

I. G. Dymnikova

A. F. Ioffe Physicotechnical Institute, Academy of Sciences of the USSR, Leningrad
Usp. Fiz. Nauk **148**, 393–432 (March 1986)

A study is made of the trajectories of free motion of test particles and photons in the Kerr metric, which describes the gravitational field of a rotating massive body. The trajectories are classified on the basis of the integrals of the motion, which have a clear physical meaning. The cases of a strong gravitational field in the neighborhood of a rotating black hole as well as the weak-field approximation describing the motion of particles in the gravitational field of a rotating star or galaxy are considered. The review includes bound states (orbits) in the field of a rotating mass, scattering and gravitational capture of particles and photons by a rotating black hole, trajectories of falling into a black hole, and the bending of light rays and the gravitational time delay of signals in the gravitational field of a rotating body.

CONTENTS

1. INTRODUCTION

In lectures read in May 1921 at Princeton University and entitled "The fundamentals of the general theory of relativity," Einstein made the following assertion: "A rotating hollow body must generate within the cavity it bounds a "Coriolis" field that deflects a body in the direction of the rotation, and also a centrifugal field... The centrifugal effect also follows from the theory, as Thirring showed." In 1918, Lense and Thirring[73] also showed that the gravitational field outside a massive rotating body must have a similar effect, tending to cause test bodies to rotate relative to a distant inertial system attached to the fixed stars. In this case, the dragging does not necessarily take place in the direction of rotation; in particular, the displacement of the perihelion of Mercury through $\Delta\Omega = 42''\,9$ in 100 years—one of the three classical general relativistic effects—must be reduced by the rotation by the amount $\Delta\Omega_{rot} \approx 4\cdot 10^{-4}\Delta\Omega$. This was the prediction and first quantitative estimate of the effect of dragging of inertial systems by the gravitational field of a rotating body.

For a long time, the Lense-Thirring effect was of purely academic interest, just like the strongly relativistic objects—the neutrons stars and black holes predicted in the framework of general relativity at the end of the thirties by Oppenheimer and his collaborators[24]—to which it has the most direct relationship. Now that neutron stars have become ordinary reality and the final confirmation of the discovery of the first black hole in the constellation Cygnus is, it seems, to be expected at any moment,[15,40] the general theory of relativity has become a working tool of astrophysical investigations.

Allowance for general relativistic effects is particularly important for the explanation of astrophysical phenomena in which black holes participate directly. According to our present ideas, such phenomena include the cosmic sources of x rays, and possibly, gamma rays, the processes responsible for the violent activity of quasars and the nuclei of galaxies, gravitational lenses, and also possible cosmic sources of gravitational radiation.

It is well known that a black hole is formed by the complete gravitational collapse of matter in situations when it cannot be withstood by the internal pressure. Qualitatively, black holes were predicted more than 200 years ago by the English physicist John Mitchell in a paper to the Royal Society in 1783. He asserted that if the Sun were shrunk so as to have a diameter ≈ 6 km, light could not leave it (references in Ref. 114). In 1799, Laplace published a paper[116] in which he gave a quantitative theory based on Newton's law. In 1939 black holes were predicted in the framework of general

 0038-5670/86/030215-23$01.80

relativity by Oppenheimer and Snyder.[24] According to modern ideas, black holes (if they exist) arise either from initial perturbations in the distribution of the matter density in the early stages in the evolution of the universe if at that time it was strongly inhomogeneous (the idea of primordial black holes was advanced by Zel'dovich and Novikov[104] in 1966. For details of their formation and subsequent fate, the reader can study the reviews of Refs. 23 and 30; the present physical and astrophysical status of primordial black holes is considered in the recent review of Ref. 107) or are the end product of the evolution of sufficiently massive stars[24] (for scenarios, see the monographs of Refs. 10 and 18) and star clusters (the idea and mechanism of formation of a massive black hole by the collapse of a collisionless system of stars were proposed in 1965 by Zel'dovich and Podurets[105]; for the subsequent development, see the review of Ref. 40 and the references given there).

The search for black holes is regarded as one of the principal tasks of the astronomy of the last decade.[29,40] It is virtually impossible to observe a black hole directly; it can be observed only through indirect manifestations associated with the influence of its strong gravitational field on the motion of the surrounding matter and on the propagation of radiation. In astrophysical models including black holes, radiation is generated in the process of heating of gas that falls into the hole and the acceleration of this gas in the accompanying magnetic field. To obtain the necessary temperature ensuring correspondence between the model and the observed picture one requires a hugh amount of energy, the source of which could be the gravitational field of the black hole. It is regarded as very probable that astrophysical black holes possess intrinsic rotation (a rotating black hole is formed naturally by the collapse of a rotating star and by the collapse of a star in a binary system). The existence of angular momentum of a black hole is required above all for quasar models, in which a centrally positioned massive (10^7–10^8 $M_\odot$) black hole must provide the energy of the radio source genetically related to the quasar—the presence of a rotating axis could preserve the "memory" of a distinguished direction during the entire lifetime of the radio source (see Ref. 40 and the references given there). In addition, the rotation of a black hole in an external field is accompanied by helpful effects analogous to unipolar induction.[108,109,115] A rotating black hole with mass M and angular momentum I in an external magnetic field H and in the presence of a constant inflow of electric charge acts as an electric battery with power (see, for example, Ref. 106 and the references given there) $W_H \approx 10^{40}(M/10^6 M_\odot)^2(I/I_{max})^2(H/10^4)^2$ erg/sec.

Investigation of the gas-dynamic and radiative processes in the vicinity of compact rotating astrophysical objects necessarily poses the question of the motion of test bodies and the propagation of radiation in the strong gravitational fields they produce. According to the general theory of relativity, test bodies[1)] move in a gravitational field along geodesics of the space—time geometry created by the distribution and motion of the matter. Geodesics are the world lines of free motion, i.e., motion governed solely by the gravitational field described by the given geometry. The timelike geodesics are the trajectories of free motion of test bodies, while the null geodesics are those of the free motion of photons, i.e., of the propagation of radiation provided its wavelength is significantly shorter than the characteristic scale of variation of the field. The space-time geometry created by a rotating massive body is described by the Kerr metric. The characteristic scale of variation of the field is determined by the radius of the event horizon: $r_+ = [1 + (1 - a^2)^{1/2}]GMc^{-2}$, where G is the gravitational constant, c is the velocity of light, M is the mass, and a is the specific dimensionless angular momentum of the gravitating body, which is related to its total angular momentum by $a = J(GM^2c^{-1})^{-1}$. If the radius of the rotating object is $r_* \gg r_+$, the Kerr metric describes the gravitational field of a rotating star or galaxy; for $r_* > r_+$ that of a neutron star, and for $r_* \to r_+$ that of a black hole.

Since particles in the neighborhood of a rotating body move along timelike geodesics of the Kerr metric, and radiation propagates along null geodesics, study of the geodesics of this metric on the one hand, gives a clear picture of the properties of the space-time geometry in the neighborhood of rotating objects and, on the other, is necessary for astrophysical applications. (There is a brief review of geodesics of the Kerr metric known up to 1979 written in the style of a guide—where what is to be found or who did what,[85] and a review of later work can be found in Ref. 112.)

The region of applicability of the geodesic approach to the study of physical processes in the neighborhood of a rotating black hole is restricted for photons by the condition that the wavelength be short compared with the characteristic scale of variation r_+ of the field; when the wavelength becomes comparable with r_+, wave effects become very important (see Ref. 112). Consideration of these questions goes beyond the scope of the present paper, but the most interesting results, associated with the phenomenon of superradiant scattering by a black hole, are briefly presented here (Sec. 2). In addition, allowance for the influence of gravitational radiation qualitatively changes the picture of the motion even in a weak field (a detailed analysis for the Schwarzschild metric is given in Ref. 10, p. 135). Quantitatively, the energy lost by a body with mass m through the emission of gravitational waves is characterized by $\alpha mc^2(m/M)$, where the coefficient α is appreciably less than unity (for the case of gravitational radiation in the field of a rotating black hole, see Ref. 6 and the references given there). Therefore, the restriction of the approximation considered below of free nonradiating particles is characterized by a quantity proportional to the ratio of the mass of the test particle to the mass of the gravitational body that produces the metric.

It should also be noted that in the present review we consider the motion of test bodies and photons in the gravitational field of a stationary black hole, i.e., it is assumed that the black hole has already been formed and that its parameters do not change. Under real astrophysical conditions, black holes are dynamical objects. They interact with the surrounding matter and fields, and the parameters which characterize them change with time. The direction that in-

vestigates the dynamical behavior of black holes in an astrophysical environment, using ideas of early studies of A. L. Zel'manov, has become particularly popular in recent years in connection with the theory of quasars. Therefore, although these questions lie outside the subject of the review, we mention briefly the fundamental principles of the dynamical description of black holes.[122] The approach is based on ascribing to a black hole a two-dimensional closed "surface," or, as it is called, a membrane. The existence of the membrane in time is represented by a timelike hypersurface, as if the membrane were an ordinary but very thin material layer. At each fixed instant of time, the membrane diameter only just exceeds the diameter of the black hole's event horizon. Like an ordinary material layer, the membrane possesses mechanical and electromagnetic properties. The layer is a viscous deformable fluid, electrically charged and conducting, and it possesses finite entropy and temperature. The equations of external electromagnetic and gravitational fields in which the black hole is situated, together with natural boundary conditions for these fields on the horizon of the black hole, determine the specific properties of the membrane and their evolution in time. This "membrane" approach to the description of the dynamical properties of black holes makes it possible to use physical intuition and ordinary astrophysical methods to analyze the interaction of a black hole with its environment.

We note also that black holes in stellar systems move in accordance with the ordinary laws of relativistic celestial mechanics. Detailed calculations for the case of binary systems are given in the studies of Ref. 123.

To construct astrophysical models directly related to observations, the geodesic motion outside the event horizon is particularly interesting. It can be divided into three types: 1) motion beginning far from the gravitating body, including the bending of light rays and the time delay of signals in the field of the rotating body and infall trajectories and gravitational capture in the field of a rotating black hole; 2) motion in finite orbits, including the effect of dragging (frame dragging) on the orbital motion; 3) the propagation of photons emitted in the vicinity of the black hole which then either reach a distant observer, or are captured by the hole, or are absorbed or scattered in the accretion disk around the hole, if there is one. Problems related to 3) are usually solved by constructing specific models of astrophysical phenomena in which the general relativistic effects are considered in conjunction with other physical (magnetohydrodynamic, radiative, etc.) effects (see the reviews of Refs. 40 and 77); their solution is based on the results obtained in 1) and 2). The influence of rotation on the propagation of radiation emitted near a black hole has been investigated "in pure form" in the problem of the formation of the image of a star on an orbit near a black hole,[57] and also in the problem of the propagation of radiation emitted in the interior optically thin regions of an accretion disk and then captured in its outer regions.[25,58,87] Such problems are solved, as a rule, numerically. (The effectiveness of various numerical methods for integrating the equations of Kerr geodesic motion is compared in Ref. 86.)

In the present paper, we consider motion of the first and second types. The numerous results, including exact analytic and numerical solutions of the geodesic equations, already obtained in this field effectively give a kinematic picture of the motion in the gravitational field of a rotating body. In it, the dragging of the inertial systems takes varied and nontrivial forms, so that one can speak of a kind of "spin-orbit" (the spin characterizes the gravitating center) interaction in the gravitational field of the rotating object. For example, the famous bending of light rays in the field of a massive body predicted by Einstein in general relativity depends in the case of the field of a rotating body on the mutual orientation of the wave vector of the photon and the rotation axis, and as a result rays with negative values of the projection of the orbital angular momentum onto the axis are deflected more strongly than rays with positive projection (Sec. 7). In the strong field of a rotating black hole, the dependence of the bending of the rays on the orientation of the orbital angular momentum relative to the axis has the consequence that photons oriented along the rotation can pass much nearer the hole than photons oriented in the opposite direction, and the cross sections for scattering and gravitational capture are strongly deformed depending on the angle of falling toward the black hole. Analogous results hold for nonrelativistic particles (Sec. 4).

The trajectories of free fall into a rotating black hole are necessarily twisted in the direction of its rotation near the hole. The radial free motion without rotation is transformed into motion in a spiral wound round the conical surface $\vartheta = \vartheta_\infty = \text{const}$. When clouds of weakly mutually interacting particles fall into a rotating black hole, their trajectories tend to collect on analogous conical surfaces $\vartheta_{1,2} = \pm \sin^{-2}\left[L_z^2/a^2(E^2-1)\right]^{1/4}$ (L_z is the projection of the angular momentum of the particle onto the axis, and E is its energy) and to twist in the direction of rotation of the hole (Sec. 5).

In the case of bound orbits, the influence of the effect of the frame dragging, or the spin-orbit interaction, leads to displacement of the periastra of the Keplerian orbits, and for spherical ($r = \text{const}$) orbits to a dragging of the nodes (the points of intersection of the orbits with the equatorial plane) in the direction of the rotation. In addition, the rotation of the central body changes the period of revolution of bodies in circular equatorial orbits, increasing the period of a direct orbit (oriented in the sense of the rotation) and decreasing the period of a retrograde orbit. As a result, the point of encounter of two test bodies moving in opposite directions around an orbit of the same radius will drift in the direction opposite to the direction of rotation of the central body (Sec. 6).

The effect of the frame dragging is manifested in a particularly interesting manner in the gravitational time delay of signals—for photons moving in the equatorial plane of a rotating object in the sense of its rotation, the additional gravitational time delay due to the rotation is negative, while for photons moving in the opposite direction it is positive. For photons falling into a rotating black hole, and also for

photons passing by any rotating object parallel to the rotation axis the additional rotational gravitational time delay is also negative! Thus, the influence of frame dragging on the propagation time of signals is manifested in the way that the gravitational time delay corresponding to rotation is often gravitational acceleration (Sec. 8).

The existence of additional gravitational time delays of opposite signs can lead to interesting consequences in situations in which a rotating massive body plays the part of a gravitational lens. In connection with recent discoveries of double and triple quasars, which are interpreted as images of the same object formed by gravitational lenses,[22,92-94] and also in connection with the discovery of extremely rapid variability in time of the radiation from certain objects in space,[75] these consequences could possibly be of practical interest. For a rotating gravitational lens, there must be a relative time delay of the rays that form the different images of the same object in the lens. In addition, it is also in principle possible to have a situation in which a rotating black hole is situated on the line of sight between the observer and an extended source of radiation and appears literally in the image of the radiation source as a black hole bounded by a curve which is not symmetric (because of the rotation) about the center and is formed by photons deflected by the black hole through angles $\Delta\varphi = \pm 3k\pi$, $k = 1, 2, 3\ldots$. In this case, there must be a relative time delay of the photons forming the luminous halo surrounding the image of the hole, and in the case of rapid variation in the brightness of the radiation source this may have the consequence that the brightness will vary nonuniformly around the halo, giving rise to a "running hare" effect (advancing spot of light) (Sec. 9).

Besides the spin-orbit interaction, there is also in the gravitational field of a rotating body a spin-spin interaction with test particles possessing intrinsic rotation. These questions lie beyond the scope of the present paper, since, strictly speaking, a particle with spin does not move along a geodesic. However, I should like to mention the most interesting effects. The first example of spin-spin interaction was given in the classical study of Lense and Thirring[73]and takes the form that an ideal gyroscope in the field of a body rotating with angular velocity ω is turned relative to a distant inertial frame associated with the fixed stars at rate $\Omega \approx \omega r_+/r$. In general relativity, the gravitational potential is not a scalar, in contrast to Newton's theory of gravitation (Ref. 10, p. 45), so that the gravitational field of a rotating body behaves like the electromagnetic field of a rotating charged body, and therefore the corresponding first-order effects are called gravimagnetic effects.[19,101] The gravitational field components, like the magnetic field of a rotating charged body, lead to a splitting of spectral lines analogous to the Zeeman effect. The gravitational Zeeman effect, predicted by Zel'dovich,[101] is universal, since the splitting does not depend on the specific properties of the radiating system and is the same over the entire range of electromagnetic waves. A line emitted at a pole with frequency ω_0 is split into two components with frequencies $\omega_0 \pm \Omega$ and with opposite circular polarizations, i.e., photons with left and right circular polarization are subject to different red shifts in the gravitational field of the rotating body.

The spin-spin interaction, like the spin-orbit interaction, depends strongly on the mutual orientation of the angular momenta. If the spin direction of the test body coincides with the direction of the rotation axis of the gravitating body, a gravitational force of repulsion arises between them; in the opposite case, there is attraction.[110] A method of experimental determination of the gravimagnetic field of the Earth was proposed by Braginskiĭ, Polnarev, and Thorne[111] on the basis of this effect.

In the gravitational field of a rotating body, there is one further form of interaction, which was predicted by Braginskiĭ and Polnarev; it is a spin-quadrupole interaction.[98] This new relativistic spin-quadrupole effect consists of the excitation of vibrations in a quadrupole mechanical oscillator in the field of a rotating gravitating body. In an orbit around the Earth, the relative amplitude of the vibrations can exceed 10^{-10}.

In the following section we write down the Kerr metric (choosing the signature as in Landau and Lifshitz[17]) and consider its most remarkable properties due to the presence of rotation: the dragging of inertial frames and the possibility of extracting from a black hole its rotational energy by: 1) the Penrose process and 2) superradiant scattering (reflection with amplification) of waves incident on the hole. The remaining sections contain a detailed review of the geodesics of the Kerr metric. Almost everywhere we use Boyer-Lindquist coordinates. These are coordinates of a distant observer that coincide asymptotically with ordinary spherical coordinates in flat space; we use the geometrical system of units ($c = G = 1$).

2. THE KERR METRIC

Although black holes are deservedly regarded as among the most exotic of the objects populating the universe, as objects they are in fact rather simple, since we can study only their external fields, which are completely determined by just three quantities, mass, charge (if present; see the review of Ref. 80), and angular momentum. This property of black holes is usually formulated as the assertion that a black hole has no "hair." For a rotating black hole. This was noted for the first time by Doroshkevich, Zel'dovich, and Novikov,[100] while the behavior of the magnetic field in the collapse process was investigated by Ginzburg.[99] (A review of later studies can be found in Ref. 18.) The Kerr metric describes the gravitational field of an uncharged rotating black hole; if the radius of a gravitating body is greater than the event horizon, it also describes in many cases the gravitational field of other rotating astrophysical objects—galaxies, stars, and neutron stars.

The metric in a given geometry characterizes the square of the distance, $ds^2 = g_{\alpha\beta}\,dx^\alpha\,dx^\beta$ ($\alpha, \beta = 0, 1, 2, 3$), between two nearby points of space-time. Considering motion in the gravitational field of a rotating body from the point of view of a distant observer, it is convenient to use Boyer-Lindquist coordinates,[42] which coincide at infinity with ordinary spherical coordinates in flat space. In these coordinates and in the geometrical system of units ($c = G = 1$), the Kerr metric takes the form

$$ds^2 = (1 - 2Mr\,\Sigma^{-1})\,dt^2 + 4M^2 ar \sin^2\vartheta \cdot \Sigma^{-1}\,dt\,d\varphi - \Sigma^{-1}\,dr^2 - \Sigma\,d\vartheta^2 - \sin^2\vartheta \times (r^2 + a^2M^2 + 2M^3a^2r \sin^2\vartheta \cdot \Sigma^{-1})\,d\varphi^2, \quad (2.1)$$

where

$$\Sigma = (-g)^{1/2} = r^2 + a^2M^2\cos^2\vartheta, \qquad \Delta = r^2 - 2Mr + a^2M^2; \quad (2.2)$$

where M is the mass of the gravitating body and a is its specific dimensionless angular momentum, which is related to the total angular momentum by $J = aGM^2c^{-1}$.

In the Kerr metric, there exist two physically distinguished surfaces: the surface S_m, on which g_{00} vanishes and which is described by the equation

$$r = r_m = M[1 + (1 - a^2\cos^2\vartheta)^{1/2}], \quad (2.3)$$

and the surface S_+, which is situated within S_m and is determined by the condition $g_{rr} \to \infty$ ($\Delta = 0$); it is described by the equation:

$$r = r_+ = M[1 + (1 - a^2)^{1/2}] \quad (2.4)$$

and is a one-sided valve or exterior event horizon of the rotating black hole.

The frame dragging effect takes the form that all locally inertial frames of reference in the gravitational field are dragged into rotation relative to a distant inertial frame. Like the field, the degree of dragging decreases with the distance, and there is therefore a differential rotation of the inertial frames with angular velocity determined in the weak-field approximation by the well-known formula of Landau and Lifshitz (Ref. 17, Vol. 2, p. 324 of the Russian original):

$$\boldsymbol{\Omega} = \frac{1}{2} g_{00}^{1/2}\ \mathrm{curl}\ \mathbf{g}, \quad (2.5)$$

where $g_i \equiv -g_{0i}g_{00}^{-1}$. In the limit of large r, the vector Ω has the components[66]

$$\Omega_r = \frac{2M^2a\cos\vartheta}{r^3}, \qquad \Omega_\vartheta = \frac{M^2a\sin\vartheta}{r^3}, \qquad \Omega_\varphi = 0. \quad (2.6)$$

Near the equatorial plane, the unit vector $\mathbf{e}^\vartheta$ is antiparallel to the angular momentum vector $\mathbf{J}$ of the central body, and therefore the rotation of the inertial frame in the equatorial plane far from the gravitating body takes place remarkably in the direction opposite to the direction of its rotation: $\boldsymbol{\Omega} \approx -\mathbf{J}r^{-3}$. It is this that leads to the decrease, mentioned above, of the advance of Mercury's perihelion and the decrease in the deflection angle of a ray passing in the equatorial plane in the direction of rotation.

In the general case of a strong field, all locally inertial frames of reference must rotate relative to the distant inertial frame with angular velocity.

$$\Omega_{\min} = -\frac{g_{0\varphi}}{g_{\varphi\varphi}} - \left(\frac{g_{0\varphi}^2}{g_{\varphi\varphi}^2} - \frac{g_{00}}{g_{\varphi\varphi}}\right)^{1/2} < \Omega < -\frac{g_{0\varphi}}{g_{\varphi\varphi}} + \left(\frac{g_{0\varphi}^2}{g_{\varphi\varphi}^2} - \frac{g_{00}}{g_{\varphi\varphi}}\right)^{1/2} = \Omega_{\max}. \quad (2.7)$$

As the surface S_m is approached, the value of $\Omega_{\min}$ increases, i.e., the frame dragging effect becomes stronger. When $g_{00} = 0$, $\Omega_{\min} = 0$; hence, all locally inertial observers are necessarily forced to rotate with positive angular velocity. Therefore, the surface S_m is the limit to the possibility of remaining static in the Kerr metric—beyond this surface, the equation $d\varphi/dt = 0$ does not have roots, so that no body within S_m can have $\varphi = \mathrm{const}$; all stationary observers (i.e., observers with $r = \mathrm{const}$ and $\varphi = \mathrm{const}$) must necessarily rotate relative to the frame of reference at rest at infinity with positive angular velocity

$$0 < \Omega < \Omega_{\max}, \quad (2.8)$$

which tends in the limit $r \to r_+$ to the angular velocity of the dragging at the horizon:

$$\Omega_+ = \frac{aM}{r_+^2 + a^2M^2}, \quad (2.9)$$

which is called the angular velocity of the rotation of the black hole.[53]

The region between the surfaces S_m and S_+ is called the ergosphere (from the Greek word $\varepsilon\rho\gamma\vartheta\eta$, meaning work). Here, events can take place accompanied by the direct extraction of rotational energy from the black hole. On the passage through the surface S_m, the component g_{00} changes sign and becomes negative. This has the consequence that in the ergosphere the energy of a particle with 4-velocity u^α, which is equal to $E = \mu(g_{00}u^0 + g_{0k}u^k)$, can be negative. The geodesics with negative E are entirely within the ergosphere, and therefore no freely moving particle can reach such a geodesic from without. However, such a geodesic can arise through the breakup of a body that enters the ergosphere, when the other fragment of the breakup can reach infinity (a distant observer) with energy $E_{\mathrm{fin}} > E_{\mathrm{in}}$, carrying away some of the rotational energy of the hole.[26,52,78] This mechanism of energy extraction from a black hole is called the Penrose process. Examples of realization of the process and possible astrophysical applications are considered in Refs. 34, 113–115, 117, 118, and 121 and in the monograph of Ref. 112.

The wave analog of the Penrose process is the superradiant scattering of waves by a rotating black hole (Refs. 11, 28, 76, 81, and 82). Such a possibility was pointed out for the first time by Zel'dovich,[102,103] who considered the scattering of electromagnetic waves by a conducting cylinder that rotates with angular velocity Ω; in this case, a wave with orbital angular momentum m and frequency ω will be amplified on reflection from the cylinder if $\omega < m\Omega$, while the energy and angular momentum of the reflecting body will be decreased. Zel'dovich showed that: 1) an analogous effect must take place for the scattering of multipole waves by a rotating black hole; 2) in the quantum treatment of scattered waves there must be spontaneous emission of energy and angular momentum through the production of pairs of photons within the ergosphere with subsequent absorption of one of them by the hole and radiation of the other to infinity, infinity corresponding to the radius of the transition from the near zone to the wave zone: $R \gtrsim cm/\omega \sim r_+$.

A more rigorous treatment shows that the wave solutions of the equations of general relativity describing perturbations on the background of the Kerr metric behave at in-

finity as $\exp[-i\omega(t \pm r_*)]$; the plus and minus signs correspond to the incoming and outgoing waves, respectively. The coordinate r_* is related to the ordinary radial coordinate r by the equation

$$\frac{dr_*}{dr} = (r^2 + a^2M^2)\,\Delta^{-1}$$

and varies in the range $-\infty < r_* < \infty$ for $r_+ \leqslant r < \infty$, and for this reason has become known as the "tortoise coordinate." In the limit $r_* \to -\infty$, the wave is described asymptotically by a function proportional to $\exp[\pm i(\omega - m\Omega_+)r_*]$, where m is the azimuthal quantum number of the wave. A physically reasonable boundary condition on the surface of the event horizon requires that the wave be incident for all local observers drifting around the hole under the influence of the frame dragging. Since such observers near the horizon must have angular velocity $\Omega \approx \Omega_+$, they will regard as incident a wave proportional to $\exp[-i(\omega - m\Omega_+)r_*]$ and having group and phase velocities $v_{gr} = -1$ and $v_{ph} = -1 + (m\Omega_+/\omega)$. It follows from this that locally the energy flux is always directed into the hole. The phase velocity, which determines the picture seen by a distant observer, can, for certain values of m and ω, be directed away from the hole. A wave incident on the black hole from infinity encounters in its path a "radial barrier," which is determined by the vanishing of the quantity $k^2(r)$ in the wave equation. The wave is partly reflected by the radial barrier and is partly absorbed by the hole. If in the incident wave $m > 0$ and the frequency lies in the interval $0 < \omega < m\Omega_+$, then for an infinitely distant observer this incident wave becomes an outgoing wave and amplifies the corresponding reflected wave mode—the wave undergoes superradiant scattering by the space-time curvature in the strong gravitational field near the rotating black hole. For a nonrotating hole, the effect is absent. From the point of view of an observer drifting around the hole, energy flows only into the hole, while from the point of view of the distant observer there is an effect of reflection with amplification—the flux of energy directed into the hole is determined for scalar waves incident on the hole by the expression[16]

$$\frac{dE}{dt} \sim \omega\,(\omega - m\Omega_+)\,\frac{2Mr_+}{4\pi}\int {}_0S^2_{lm}(\vartheta)\sin\vartheta\,d\vartheta\,d\varphi_0,$$

where ${}_0S_{lm}(\vartheta; a\omega)$ are angular functions corresponding to the symmetry of the problem: spheroidal wave harmonics (see, for example, Refs. 6 and 32 and the references given there). For $0 < \omega < m\Omega_+$, the derivative dE/dt becomes negative, i.e., energy is extracted from the hole and carried away to infinity. Similar but more complicated expressions can be found for electromagnetic and gravitational waves.[28] The coefficient of reflection of electromagnetic waves exceeds unity by a few percent and reaches a maximum in the limit $\omega \to m\Omega_+$. The characteristic frequencies are $\omega \sim 0.5c^3(GM)^{-1}$ and in the case of black holes of a stellar mass and more lie in the radio range. A gravitational wave can be amplified by more than a factor 2—the reflection coefficient is $R_{gr} = 2.38$ for $a \to 1$, $l = m = 2$, and $\omega \to m\Omega_+$.[28,82]

The amplification of gravitational waves reflected in the strong gravitational field of a rotating black hole leads to the possibility of the existence in its neighborhood of so-called floating orbits, in which the energy losses through the emission of gravitational waves are completely compensated by the energy extracted from the hole by the superradiant scattering.[76,81]

The superradiant scattering of electromagnetic waves is the basis of the idea of a "black hole bomb,"[81] which exploits the possibility, first pointed out by Zel'dovich,[103] of multiple amplification of radiation by the introduction of a positive feedback realized by a spherical mirror that is placed optimally around a rotating black hole and reflects low-frequency radio waves.

3. INTEGRALS OF THE MOTION

The equations satisfied by the motion of test particles in the Kerr metric can be obtained from the Hamilton-Jacobi equations

$$g^{\alpha\beta}\frac{\partial S}{\partial x^\alpha}\frac{\partial S}{\partial x^\beta} - \mu^2 = 0 \qquad (\alpha, \beta = 0, 1, 2, 3),$$

the action being written in the form

$$S = -Et + L_z\varphi + S_r(r) + S_\vartheta(\vartheta).$$

As a result, one obtains equations of motion[50] that are the first integrals of the geodesic equations:

$$\Sigma^2\dot{r}^2 = R(r)$$

$$\equiv [E(r^2+a^2) - aL_z]^2 - \Delta[\mu^2r^2 + Q + (L_z - aE)^2], \tag{3.1}$$

$$\Sigma^2\dot{\vartheta}^2 = Q - H(\vartheta) \equiv Q - \cos^2\vartheta\left[a^2(\mu^2 - E^2) + \frac{L_z^2}{\sin^2\vartheta}\right], \tag{3.2}$$

$$\Sigma\dot{\varphi} = \frac{L_z}{\sin^2\vartheta} - aE + \frac{a}{\Delta}[E(r^2+a^2) - aL_z], \tag{3.3}$$

$$\Sigma\dot{t} = a(L_z - aE\sin^2\vartheta) + \frac{r^2+a^2}{\Delta}[E(r^2+a^2) - aL_z]; \tag{3.4}$$

here, μ is the rest mass of the particle, the dot denotes differentiation with respect to the affine parameter λ, which is related to the proper time by the equation $\tau = \mu\lambda$; for a photon $\mu = 0$. The coordinates r and t are measured by a distant observer in units of GMc^{-2} and GMc^{-3}. The quantities Q, E, and L_z are integrals of the motion, the significance of which can be elucidated by means of the passage to the limit $r \to \infty$:

$$\left(\frac{dr}{dt}\right)_\infty^2 + r^2\left(\frac{d\vartheta}{dt}\right)_\infty^2 + r^2\sin^2\vartheta_\infty\left(\frac{d\varphi}{dt}\right)_\infty^2 = \frac{E^2-\mu^2}{E^2} = v_0^2, \tag{3.5}$$

$$Er^2\sin^2\vartheta_\infty\left(\frac{d\varphi}{dt}\right)_\infty = L_z, \tag{3.6}$$

$$Q + L_z^2 = L^2 - a^2(E^2-\mu^2)\cos^2\vartheta_\infty. \tag{3.7}$$

In the case of a nonrotating body, the Kerr metric becomes the Schwarzschild metric, and $Q + L_z^2$ is the square of the total conserved angular momentum of the test body. At the same time, the integral Q is related to the Laplace vector, which arises on the transition to the Kepler problem in the Newtonian theory of gravitation.

Thus, E is the conserved energy of the test particle, L_z is the conserved projection of the angular momentum onto the rotation axis, L is the total initial angular momentum, and v_0 is the initial velocity of the particle.

The quantities μ, E, and L_z are three obvious integrals of the motion in the Kerr metric. The existence of the fourth integral Q was initially somewhat unexpected (see, for example, Ref. 18). However, papers were soon published in which its existence was justified from the mathematical point of view.[2)] The point is that in the language of differential geometry the existence of integrals of the motion is associated with the existence in the given geometry of Killing vectors, which describe infinitesimally small translations in space-time that preserve curve length (see, for example, Ref. 18). If the metric $g^{\alpha\beta}$ does not depend on a certain coordinate x^α, then the Killing vector $\xi = \mathrm{d}/\mathrm{d}x^\alpha$, which satisfies the Killing equation $\xi_{\beta;\nu} + \xi_{\nu;\beta} = 0$, describes the symmetry of space-time with respect to the coordinate shift $x^\nu \to x^\nu + \varepsilon\delta^\nu_\alpha = x^\nu\ \varepsilon\xi^{\ \nu}_{\alpha}$ along the cyclic coordinate x^α. Under such a curve-length conserving transformation, the distances between the space-time points remain the same, i.e., the geometry is not changed. To each Killing vector there corresponds a quantity that is conserved in free motion, i.e., motion along a geodesic, it is $\xi^\nu t_\nu$, where $t_\nu = \mathrm{d}x_\nu/\mathrm{d}\lambda$ is the vector tangent to the geodesic and normalized such that $t^\alpha t_\alpha = -\mu^2$. In the Kerr metric, the coordinates t and φ are cyclic, and there are the two Killing vectors $\xi^\alpha = \delta^\alpha_t$ and $\zeta^\alpha = \delta^\alpha_\varphi$, to which correspond the conserved quantities $E = -\xi^\nu t_\nu$ and $L_z = \zeta^\nu t_\nu$. They are identified with the energy and the projection of the angular momentum onto the rotation axis, since asymptotically as $r \to \infty$ the Killing vector ξ^α corresponds to the generator of displacements in time and ζ^α to the generator of rotations about the symmetry axis. Both these integrals of the motion are linear in the components of the tangent vector and, therefore, in the components of the momentum and angular momentum.

It was found[56,68,69,91] that in the Kerr metric there are not only the Killing vectors but also a Killing tensor $K_{\alpha\nu}$, a symmetric second-rank tensor related to the angular momentum of the field source and satisfying the equation $K_{\alpha\nu;\sigma} + K_{\alpha\sigma;\nu} = 0$. Because of this, there exists a quadratic integral of the motion $K = K_{\alpha\nu} t^\alpha t^\nu$ conserved in free motion and related to our integral of the motion Q by the identity transformation $Q + (L_z - aE)^2 \equiv K$. On the transition to the Schwarzschild metric, K becomes the square of the total angular momentum of a test particle, which is conserved in the case of motion in spherically symmetric geometry. For motion in the equatorial plane of a rotating body $Q + L_z^2$ also formally has the meaning of the square of the total angular momentum, but, as follows from Eqs. (3.3) and (3.4), in this case $Q \equiv 0$. One could expect that this quantity would tend to the square of the total angular momentum of the particle as $r \to \infty$, since the Kerr metric is asymptotically flat. However, as follows from (3.7), this does not occur, and the effect can be interpreted as a coordinate effect,[64] i.e., as the result of describing space-time by coordinates that lead to the additional a^2-dependent term in (2.7), which describes at infinity a fictitious contribution to the angular momentum of the particle due to the noninertial nature of the coordinate system or, equivalently, the angular momentum of the gravitational field itself.

Thus, the geodesic of a particle in the Kerr metric is completely determined by its integrals of the motion E, L_z, and Q. Some general properties of geodesics follow from an analysis of the first integrals (3.1)–(3.4) by the method of effective potentials.[50,14,95] Writing the expression for the right-hand side $R(r)$ of Eq. (3.1) in a form that does not depend on the mass μ of the particle, i.e., regarding E and L_z as specific quantities, we obtain

$$R(r) = (E^2-1)\, r^4 + 2r^3 + 2\,[a^2(E^2-1) - L_z^2 - Q]\, r^2 + 2\,[Q + (L_z - aE)^2]\, r - a^2 Q. \qquad (3.8)$$

From the form of the coefficient of r^4 we obtain an obvious condition—no geodesic can reach infinity if the corresponding energy satisfies $E^2 < 1$. In this case, the motion is bounded, or finite, i.e., the particle moves in a region bounded with respect to r and neither reaches infinity nor intersects the event horizon (if gravitational radiation is taken into account, the picture is changed: The particle, radiating gravitational waves, will gradually approach the event horizon, going over to ever closer orbits until it is captured by the hole).

The effective potentials are determined as solutions of the equation

$$R(r) = [r^4 + a^2(r^2+2r)]\, E^2 - 4arL_zE + L_z^2a^2 - (r^2 + Q - L_z^2)\,\Delta = 0. \qquad (3.9)$$

They have the form

$$U_\pm(r,\ L_z,\ Q) = \frac{4aL_zr \pm D^{1/2}}{2\,[r^4 + a^2(r^2+2r)]}, \qquad (3.10)$$

where D is the discriminant of Eq. (3.9), and they are shown in Fig. 1 (Ref. 14) for the case of an extremely rotating ($a = 1$) black hole. The asymptotic behavior of $U_\pm$ and their derivatives is determined by[14]

$$U_\pm \xrightarrow[r\to r_+]{} \frac{aL_z}{2r_+}, \quad U_\pm \xrightarrow[r\to\infty]{} \pm 1, \quad \frac{\partial U_\pm}{\partial r} \xrightarrow[r\to r_+]{} \pm\infty, \quad \frac{\partial U_\pm}{\partial r} \xrightarrow[r\to\infty]{} 0. \qquad (3.11)$$

For reality of the radial velocity $\dot{r}$, non-negativity of the function $R(r)$ is required, i.e., fulfillment of the conditions

$$E \geqslant U_+(r,\ L_z,\ Q), \qquad (3.12a)$$

$$E \leqslant U_-(r,\ L_z,\ Q), \qquad (3.12b)$$

which are related by a one-to-one correspondence: E, L_z, $Q \leftrightarrow -E$, $-L_z$, Q, as can be seen in Fig. 1. Bound states arise in the region of energies in which there exist not less than three points of intersection of the curve $U_+(r, L_z, Q)$ with the straight line $E = \mathrm{const}$ (turning points of the particle trajectory). Analysis of the number of sign alternations in the expression (3.9) shows that in the region of energies $E^2 \geqslant 1$ there can exist not more than two turning points, and in the region $E^2 < 1$ not more than three (see Fig. 2, Ref. 14).

The condition for the motion to be finite, $E^2 < 1$, immediately imposes on the integral of the motion Q restrictions that can be obtained by writing the right-hand side of Eq. (3.2)—the latitude potential $Q - H(\vartheta)$—in the form[95]

$$Q - H(\vartheta) = a^2\cos^2\vartheta\,(E^2 - V^2(\vartheta)),$$

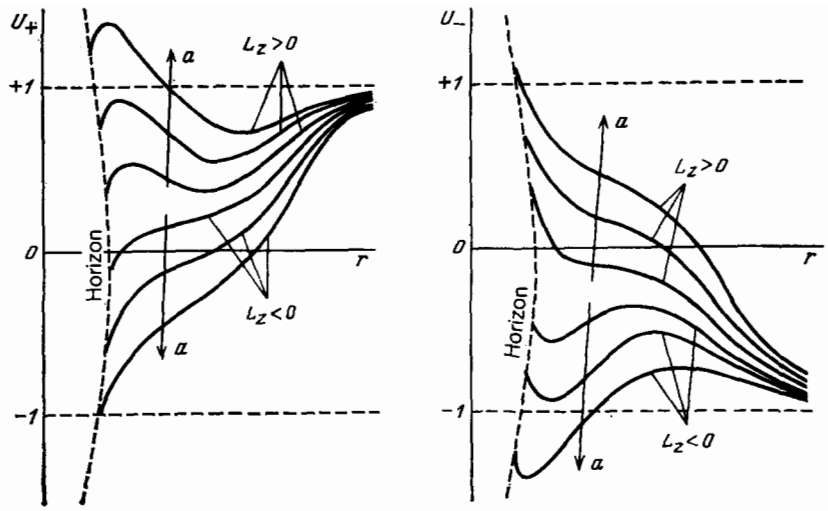

FIG. 1. Effective radial potentials $U_+(r, L_z, Q)$.

where

$$V^2(\vartheta)=1+\frac{1}{a^2}\left(\frac{L_z^2}{\sin^2\vartheta}-\frac{Q}{\cos^2\vartheta}\right).$$

The condition $E^2-V^2(\vartheta)\geqslant 0$ for all values of L_z in the region of values $E^2<1$ presupposes positivity of Q. For if $Q<0$, then $V^2(\vartheta)>1$ and $E^2>1$. Thus, bound states are possible only for $Q\geqslant 0$ and $E^2<1$, and the orbit is characterized by the value $Q=0$ if and only if it is restricted to the equatorial plane. This can be readily seen by considering the behavior of the latitude potential $H(\vartheta)$ for $E^2<1$ (Fig. 3, Ref. 14). All finite motions with $Q<0$ are forbidden by Eq. (3.2), since $Q<0$ would imply negativity of $\dot{\vartheta}^2$. The only point on the curve $H(\vartheta)$ characterizing motion with $\vartheta=\text{const}$ corresponds to the value $\vartheta=\pi/2$, i.e., to finite orbits in the equatorial plane. Nonequatorial finite orbits with $\vartheta=\text{const}$ do not exist in the Kerr metric[14,62]; finite circular ($r=\text{const}$) orbits on the surface $\vartheta=\text{const}$ could exist in the field of a charged rotating black hole, for which the equilibrium of the particle in the orbit is ensured by the competing effect of the electromagnetic and gravitational forces (see, for example, Refs. 46 and 63 and the review of Ref. 80).

The condition $Q\geqslant 0$ is a necessary but not sufficient condition for finite motion. For $Q\geqslant 0$, there exist both finite as well as infinite trajectories of free motion. For $Q<0$, all the admissible geodesics are infall trajectories, if the particle initially moves along the direction toward the hole, the particle being necessarily, as it approaches the hole, dragged into rotation around the axis in the direction of rotation of the hole (see Sec. 5).

Thus, all trajectories of free motion can be divided into two classes depending on the sign of Q.[14,46,48] Geodesics of the first class have $Q\geqslant 0$. They intersect the equatorial plane or are entirely situated in it (for $Q=0$) and are called geodesics of orbital type.[46] Geodesics of the second class have $Q<0$ and never intersect the equatorial plane; when

$$\begin{aligned} K&>-2aL_z[E-(E^2-1)^{1/2}]+a^2 \quad \text{for} \quad L_z>0,\\ K&>-2aL_z[E+(E^2-1)^{1/2}]+a^2 \quad \text{for} \quad L_z<0 \end{aligned} \tag{3.13}$$

particles move between two hyperboloids $\vartheta=\text{const}<\pi/2$ (Refs. 46 and 61) in giant vortices, since $\varphi=\text{const}$ is impossible near the hole. These geodesics are called geodesics of vortical type.[46] In the special case when

$$K=-2aL_z[E-(E^2-1)^{1/2}]+a^2 \quad \text{for}$$
$$\times 0<L_z<a(E^2-1)^{1/2}, \tag{3.14}$$
$$K=-2aL_z[E+(E^2-1)^{1/2}]+a^2 \quad \text{for}$$
$$-a(E^2-1)^{1/2}<L_z<0,$$

the motion takes place along the surface of the hyperboloid $\vartheta_{1,2}=\text{const}$, where $\vartheta_{1,2}=\pm\sin^{-1}[L_z^2/a^2(E^2-1)]^{1/4}$, and is stable with respect to ϑ perturbations.[14,61] The separation of the geodesics into the two indicated types is shown for the case of photons in Fig. 4 (Ref. 48): the region of motion of vortical type is bounded by the conditions

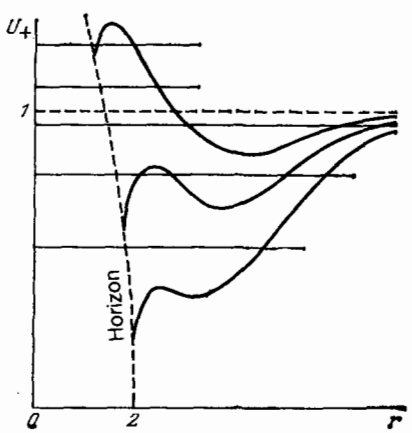

FIG. 2. Radial motion is unbounded for $E^2>1$.

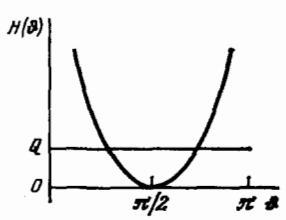

FIG. 3. Latitude potential $H(\vartheta)$ for the case $E^2<1$.

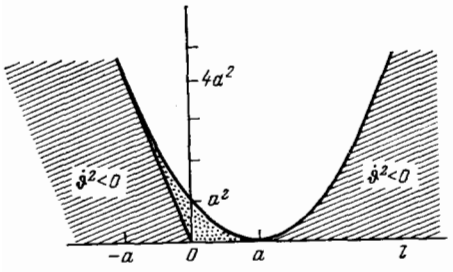

FIG. 4. Division of geodesic motion into orbital and vortical depending on the integrals of the motion K and L_z.

$$Q\leqslant 0 \quad \text{or} \quad K\leqslant (L_z-aE)^2, \qquad K\geqslant 0, \quad -a\leqslant \frac{L_z}{E}\leqslant a \tag{3.15}$$

and in Fig. 4 is filled with dots. The region of motion of orbital type is situated within the parabola $K=(L_z-aE)^2$. In all the remaining range of K and L_z/E values, motion is forbidden ($\dot{\vartheta}^2<0$). Points situated on the parabola $K=(L_z-aE)^2$ itself describe motion in the equatorial plane.[14,45]

The integral of the motion L_z determines the possibility of reaching the poles and the rotation axis in free motion. For $L_z\neq 0$, as follows from Eq. (3.2), the geodesic of a particle never reaches the poles; this is possible only for $L_z=0$. A particle can move along the axis only if[49]

$$L_z=0, \qquad Q=-a^2(E^2-1). \tag{3.16}$$

Motion along the axis is always unbounded in the radial direction, since turning points in the equation $R(r)=0$ appear only at negative values of r:

$$r_t=-1+[1-a^2(E^2-1)]^{1/2}.$$

The condition $L_z=0$ is only a necessary condition for the reaching of the poles or the rotation axis. In the general case with $L_z=0$ there exist geodesics with polar angle ϑ not equal to 0 or π. A characteristic feature of such geodesics is the monotonic variation of the azimuthal angle $\varphi(\tau)$ along the trajectory in accordance with the equation

$$\varphi=\frac{2aEr}{\Delta(r^2+a^2\cos^2\vartheta)}, \tag{3.17}$$

in complete agreement with the dragging of the inertial frames by the gravitational field of the rotating body. Another feature is the fact that the region of variation of the polar angle ϑ is restricted to one of the hemispheres (see Sec. 5).

4. SCATTERING AND GRAVITATIONAL CAPTURE

4.1. Impact parameters

Scattering by a rotating center is characterized by two impact parameters (Fig. 5), which are related to the integrals of the motion, the initial value ϑ_0 of the polar angle, and the initial particle velocity v_0 by

$$\rho_\perp=\frac{1}{v_0}r^2\sin^2\vartheta_0\left(\frac{d\varphi}{dt}\right)_\infty=\frac{L_z}{Ev_0\sin\vartheta_0}, \tag{4.1}$$

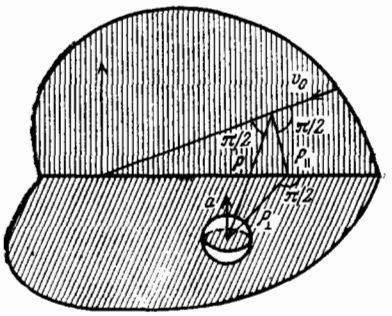

FIG. 5. Impact parameters for scattering by a rotating center.

$$\rho_\parallel=\frac{1}{v_0}r^2\left(\frac{d\vartheta}{dt}\right)_\infty =\pm\frac{1}{Ev_0}(Q+a^2E^2v_0^2\cos^2\vartheta_0-L_z^2\operatorname{ctg}^2\vartheta_0)^{1/2}.$$

They can be either positive or negative. Negativity of the impact parameter $\rho_\perp$ means that the component L_z of the orbital angular momentum of the particle is opposite in direction to the angular momentum of the hole. The sign of $\rho_\parallel$ is determined by the initial variation of the polar angle ϑ. In their turn, the components L_z and Q and the total angular momentum L can be expressed in terms of $\rho_\perp$ and $\rho_\parallel$ by

$$\begin{aligned} Q+L_z^2&=E^2v_0^2\rho^2-a^2(E^2-\mu^2)\cos^2\vartheta_0,\\ L_z&=\rho_\perp v_0E\sin\vartheta_0,\\ L&=Ev_0\rho=Ev_0(\rho_\perp^2+\rho_\parallel^2)^{1/2}. \end{aligned} \tag{4.2}$$

The coordinate of a turning point of a trajectory is found as a root of Eq. (3.1), which describes the radial motion. In the case of scattering by a black hole, it is possible to have gravitational capture of an incident particle by the hole, and therefore all the infinite orbits beginning far away from the black hole are divided into capture or infall orbits and escape orbits. In addition, there are intermediate orbits corresponding to capture by an unstable orbit in the neighborhood of the hole; from the formal point of view, they are not capture orbits but can become such when allowance is made for dissipative processes.

In the case of radial motion toward the hole, when the angular momentum and both impact parameters are equal to zero, capture is unavoidable, the rotating black hole forcing the particle, before swallowing it, to twist in the direction of its rotation (see Sec. 5). In this case, the equation $R(r)=0$ does not have real roots for $r\geqslant r_+$. When the angular momentum of the incident particle is increased to a certain critical value, the first root (which is double) appears; this determines the position of an extremum of the function $R(r)$ and the radius of the unstable spherical orbit that separates the infall orbits from the escape orbits. With further increase in the angular momentum of the particle, the function $R(r)$ acquires two real roots, at least one of which lies in the region $r>r_+$, corresponding to the appearance of escape orbits. To the limiting unstable spherical orbit correspond critical values of the impact parameters; a particle with nearly critical impact parameters passes many times around the hole before escaping to infinity or falling into the hole (for this situation there are analogies both in classical scattering theory—the orbiting effect associated with falling into a Newtonian sin-

gular potential $\sim r^{-3}$—as well as in quantum mechanics—resonance scattering).

4.2. Nonrelativistic particles

For nonrelativistic ($v_0 \ll 1$) particles, the coordinate of a turning point is determined as solution of the equation

$$r^3 - \frac{1}{2} v_0^2 (\rho^2 - a^2 \cos^2 \vartheta_0) r^2 + (v_0^2 r^2 + a^2 - 2\rho_\perp v_0 a \sin \vartheta_0) r$$

$$- \frac{1}{2} v_0^2 a^2 (\rho^2 - a^2 - \rho_\perp^2 \sin^2 \vartheta_0) \equiv f(r) = 0. \quad (4.3)$$

For particles incident in the equatorial plane, $Q = 0$ and $\rho_\parallel = 0$, and the critical values of the impact parameter $\rho_\perp$ corresponding to falling with positive and negative angular momentum L_z are[4,84,26]

$$\rho_\perp^{(+)} = \frac{2}{v_0} [1 - (1-a)^{1/2}], \quad \rho_\perp^{(-)} = -\frac{2}{v_0} [1 + (1-a)^{1/2}]. \quad (4.4)$$

The minimal value $r_{\min}$ of the distance of closest approach

$$r_0 = 2 \mp a + 2(1 \mp a)^{1/2} \quad (4.5)$$

is simultaneously the radius of the limiting unstable circular equatorial orbit and the minimal periastron of the escape orbits. For an extremal ($a = 1$) Kerr black hole $r_0 = 1$ for $\rho_\perp^{(+)}$ and $r_0 = 5.83$ for $\rho_\perp^{(-)}$.[34,35] A particle falling into the hole with negative impact parameter $\rho_\perp$ can initially encounter a turning point with respect to φ[74]: $r_\varphi = 2[1 - (aE/L_z)]$, and it then changes the direction of its orbital motion before capture.

Particles falling in the equatorial plane with impact parameters $\rho > \rho_{\text{crit}}$ pass around the black hole and go away to infinity in parabolic (for $v_0 \ll 1$, to good accuracy $E = \mu$) orbits with periastron[97]

$$r_p = \frac{\rho_\perp^2}{4} \left\{ 1 + \left[1 - \frac{16(\rho_\perp - a)^2}{\rho_\perp^4} \right]^{1/2} \right\}. \quad (4.6)$$

The angle of deflection of particles in the equatorial plane of a rotating body is determined in the weak-field approximation ($r_p \gg r_+$) by the expression[41] (here, we have taken into account the dependence, not considered in Ref. 41, of the deflection angle on the sign of the orbital angular momentum of the particle)

$$\theta \equiv \Delta\varphi - \pi = 2 \frac{(2\gamma^2 - 1)}{|\rho_\perp| (\gamma^2 - 1)^{1/2}} + \left[\frac{3\pi}{4} (5\gamma^2 - 1) - 4\gamma a (\gamma^2 - 1)^{1/2} \frac{\rho_\perp}{|\rho_\perp|} \right] \frac{1}{\rho_\perp^2},$$

$$\gamma = \frac{1}{(1 - v_0^2)^{1/2}},$$

and in the small-angle approximation the differential cross section of scattering, with allowance for the sign of $\rho_\perp$ (L_z), has the form

$$\frac{d\sigma}{d\Omega} = \left[\frac{2(2\gamma^2 - 1)}{\theta^2 (\gamma^2 - 1)} \right]^2 + \frac{3\pi (5\gamma^2 - 1)}{4\theta^3 (\gamma^2 - 1)} - \frac{4\gamma a}{\theta^3 (\gamma^2 - 1)^{1/2}} \frac{\rho_\perp}{|\rho_\perp|}.$$

The first term corresponds to Rutherford's formula for scattering by a gravitational potential $\sim 1/r$, the second gives the general relativistic correction, which does not depend on the rotation (see also Ref. 55), while the third term describes the influence of the rotation of the scattering center, giving an essentially asymmetric picture of the scattering.

For particles incident parallel to the rotation axis, $L_z = 0, \rho_\perp = 0$, and the function $f(r)$ takes the form

$$f(r) = r^3 - q \frac{r^2}{2} + (q + a^2) r - q \frac{a^2}{2},$$

where $q \equiv v_0^2 (\rho_\parallel^2 - a^2)$. The position of the turning point of the trajectory is determined as

$$r_{\min} = \frac{1}{6} [q + (q^2 - 12q - 12a^2)^{1/2}]$$

for all $q \geqslant q_0$, where q_0 satisfies the equation

$$(1 - a^2) q_0^4 + 4(5a^2 - 4) q_0^3 - 8a^2 (6 + a^2) q_0^2 - 48a^4 q_0 - 16a^6 = 0$$

and corresponds to the impact parameter of capture and to the radius of the limiting unstable spherical orbit. For $a = 1$, the scattering is characterized by the following values of the critical impact parameter, the minimal periastron, and the cross section of gravitational capture:

$$\rho_\parallel^{\text{crit}} = 3{,}85 \frac{c}{v_0}, \quad r_0 = 3{,}37M, \quad \sigma_\parallel = 14{,}8\pi \left(\frac{c}{v_0} \right)^2. \quad (4.7)$$

These expressions are also valid for arbitrary angles of incidence ϑ_0 provided that the projection of the angular momentum of the particle onto the axis is not too large; the corresponding restrictions have the form

$$\sin^2 \vartheta_0 \ll 1 + \frac{\rho_\parallel^2}{\rho_\perp^2}, \quad a\rho_\perp \sin \vartheta_0 \ll \rho^2 \frac{v_0^2}{2}$$

and are not satisfied only for large values of $\rho_\perp$ in the case of incidence at angles ϑ_0 near $\pi/2$. The cross sections for gravitational capture of a flux perpendicular to the axis and of an isotropic flux are respectively[97]

$$\sigma_\perp = 14{,}2\pi \left(\frac{c}{v_0} \right)^2, \quad \sigma_{\text{is}} = 14{,}4\pi \left(\frac{c}{v_0} \right)^2. \quad (4.8)$$

Comparison of the cross sections (4.7) and (4.8) shows that the gravitational capture of nonrelativistic particles takes place most effectively in the case of incidence parallel to the rotation axis.

4.3. Photons and ultrarelativistic particles

The scattering of ultrarelativistic particles and photons whose wavelength is much less than the radius of the event horizon is described by Eqs. (3.1)–(3.4) with $v_0 \to 1$ and $E \to \infty$. Then the integrals of the motion Q and L_z increase unboundedly, but L_z/E and Q/E^2 remain finite and can be interpreted as the impact parameters introduced above. The condition for the presence of a turning point in a photon trajectory is

$$(r^2 + a^2 - a\rho_\perp \sin \vartheta_0)^2 - \Delta [\rho_\parallel^2 + (\rho_\perp - a \sin \vartheta_0)^2] = 0. \quad (4.9)$$

For incidence in the plane of the equator $\rho_\parallel = 0$, and the critical values of the impact parameter $\rho_\perp$ are determined from the equation[66]

$$(\rho_\perp + a)^3 - 27 (\rho_\perp - a) = 0,$$

whose solutions can be written in the form[10]

$$\rho_\perp^{(+)} = a + 8 \cos^3 \left[\frac{1}{3} (\pi - \cos^{-1} |a|) \right] \quad (4.10)$$

for incidence with positive angular momentum L_z and in the form

$$\rho_{\perp}^{(-)} = a - 8\cos^3\left(\frac{1}{3}\cos^{-1}|a|\right) \tag{4.11}$$

for incidence with negative angular momentum L_z. The corresponding unstable circular photon orbit has the radius[35]

$$r_{ph} = 2\left\{1 + \cos\left[\frac{2}{3}\cos^{-1}(\mp a)\right]\right\} \tag{4.12}$$

and the angular momentum in the orbit

$$\frac{L_z}{E} = \pm\frac{1}{2}r_{ph}^{1/2}(r_{ph}+3). \tag{4.13}$$

The upper sign corresponds to a direct orbit (the direction of the orbital angular momentum is the same as the direction of rotation of the black hole), and the lower to a retrograde orbit (these directions opposite). When $a = 1$, $r_{ph} = 1$ and $\rho_{\perp} = 2$ for a direct orbit and $r_{ph} = 4$ and $\rho_{\perp} = -7$ for a retrograde orbit.[35] Examples of photon geodesics in the equatorial plane are given in Fig. 6 (Ref. 54). It can be clearly seen how the rotation of the hole destroys the symmetry between the orbits with positive and negative parameters—a photon with impact parameter $\rho_{\perp} = -8$ is deflected much more strongly than one with $\rho_{\perp} = +8$. All captured photons with negative impact parameters change in the process of capture the direction of their orbital motion under the influence of the dragging by the gravitational field of the rotating black hole.

In the case of incidence with arbitrary initial angle ϑ_0, the range of values of the impact parameters of photons captured by the hole is bounded in the case $a = 1$ by the curve[8]

$$\rho_{\parallel}^2 + (\rho_{\perp} - \sin\vartheta_0)^2 - 4[\rho^2 + (\rho_{\perp} - \sin\vartheta_0)^2]^{1/2} + 4(\rho_{\perp}\sin\vartheta_0 - 1) = 0. \tag{4.14}$$

Photons that come within this curve are captured at the points

$$r_0 = \frac{1}{2}[\rho_{\parallel}^2 + (\rho_{\perp} - \sin\vartheta_0)^2]^{1/2} \equiv \frac{\tilde{\rho}}{2}; \tag{4.15}$$

the remaining photons are deflected at the points

$$r_{min} = \frac{1}{2}\{\tilde{\rho} + [\tilde{\rho}^2 - 4\tilde{\rho} + 4(\rho_{\perp}\sin\vartheta_0 - 1)]^{1/2}\}. \tag{4.16}$$

For photons incident parallel to the rotation axis,

$$r_{min} = \frac{1}{2}[\rho_{\parallel} + (\rho_{\parallel}^2 - 4\rho_{\parallel} - 4)^{1/2}], \qquad \rho_{\parallel}^{crit} = 2(1+\sqrt{2}), \tag{4.17}$$
$$r_0 = 1 + \sqrt{2}, \quad \sigma_{\parallel} = 23.31\pi.$$

The cross sections of gravitational capture for a flux of photons perpendicular to the axis and for an isotropic flux are, respectively,[97]

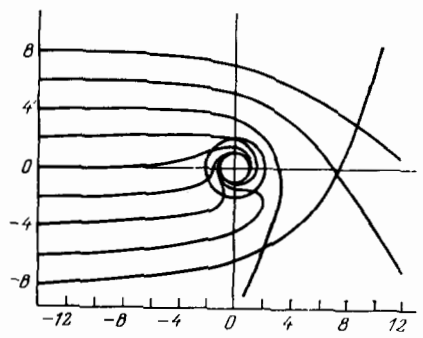

FIG. 6. Photon geodesics in the equatorial plane.

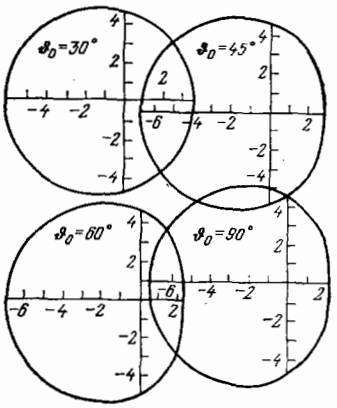

FIG. 7. Dependence of shape of the gravitational capture cross section on the angle of incidence for the case of an extremal black hole.

$$\sigma_{\perp} = 24.27\pi, \qquad \sigma_{is} = 23.90\pi. \tag{4.18}$$

Comparison of (4.17) and (4.18) shows that, in contrast to nonrelativistic particles, photons and ultrarelativistic particles are most effectively captured by a rotating black hole in the case of incidence perpendicular to the rotation axis.

As for particles, the photon capture cross section depends weakly on the angle of incidence. However, the shape of the capture cross section depends strongly on the angle. For incidence at angle $\vartheta_0 \neq 0$, particles and photons with positive L_z can pass much closer to the hole than photons and particles with negative L_z, so that with increasing angle of incidence the capture cross section becomes more and more asymmetric. Figure 7 shows how the shape of the cross section of photon gravitational capture depends on the angle of incidence. The cross section is maximally asymmetric in the case of incidence perpendicular to the axis.[35,97,7] In this case, photons with impact parameters

$$|\rho_{\parallel}| \leqslant 3\sqrt{3}, \qquad -7 \leqslant \rho_{\perp} \leqslant 2 \tag{4.19}$$

are captured at the points

$$r_0 = \frac{1}{2}[\rho_{\parallel}^2 + (\rho_{\perp} - 1)^2]^{1/2}. \tag{4.20}$$

For angles of incidence in the interval

$$\sin^{-1}(\sqrt{3}-1) \leqslant \vartheta_0 \leqslant \frac{\pi}{2},$$

the capture cross sections have a straight section, which represents the capture of photons with impact parameters

$$\rho_{\perp} = \frac{2}{\sin\vartheta_0}, \qquad \rho_{\parallel} \leqslant \left[4 - \left(\frac{2}{\sin\vartheta_0} - \sin\vartheta_0\right)^2\right]^{1/2}$$

directly at the point $r_0 = r_+$.

The characteristics of the scattering of particles and photons by an extremal black hole are shown in Table I. The curious features in the behavior of the capture cross section with increasing angle of incidence (increase for photons and decrease for particles; see Table I) can be explained by the effect of the dragging of the inertial frames. Outside the rotating body, the angular velocity (2.5) of the inertial system, written down at the given point in the local basis of unit vectors along dr, $d\vartheta$, $d\varphi$, has the form

$$\Omega = -\frac{1}{g_{00}^{1/2}}\frac{g_{0\varphi}}{g_{\varphi\varphi}}\left(\cos\vartheta\cdot\mathbf{e}^r + \frac{1}{2g_{00}^{1/2}}\sin\vartheta\cdot\mathbf{e}^{\vartheta}\right). \tag{4.21}$$

TABLE I. Characteristics of the scattering of particles and photons by an extremally rotating black hole.

Angle of incidence	Impact parameters of capture	Distance of closest approach	Cross section of gravitational capture
	Particles		
$\sin^2\vartheta_0 \ll 1+\frac{\rho_{\parallel}^2}{\rho_{\perp}^2}$	$3{,}85\frac{c}{v_0}$	3,37	$14.8\pi\left(\frac{c}{v_0}\right)^2$
90°	$\lvert\rho_{\parallel}\rvert\leqslant 3{,}85\frac{c}{v_0}$, $-4{,}8\frac{c}{v_0}\leqslant\rho_{\perp}\leqslant 2\frac{c}{v_0}$	$1\leqslant d\leqslant 5{,}83$	$14.2\pi\left(\frac{c}{v_0}\right)^2$
Isotropic flux			$14.4\pi\left(\frac{c}{v_0}\right)^2$
	Photons		
0°	$2(1+\sqrt{2})$	$1+\sqrt{2}$	$23{,}31\pi$
30°	$\lvert\rho_{\parallel}\rvert\leqslant 4{,}94$, $-6\leqslant\rho_{\perp}\leqslant 3{,}5$	$1{,}5\leqslant d\leqslant 3{,}23$	$23{,}56\pi$
45°	$\lvert\rho_{\parallel}\rvert\leqslant 5{,}04$, $-6{,}4\leqslant\rho_{\perp}\leqslant 2{,}8$	$1{,}06\leqslant d\leqslant 3{,}55$	$23{,}66\pi$
60°	$\lvert\rho_{\parallel}\rvert\leqslant 5{,}12$, $-6{,}73\leqslant\rho_{\perp}\leqslant 2{,}31$	$1\leqslant d\leqslant 3{,}80$	$23{,}80\pi$
90°	$\lvert\rho_{\parallel}\rvert\leqslant 3\sqrt{3}$ $-7\leqslant\rho_{\perp}\leqslant 2$	$1\leqslant d\leqslant 4$	$24{,}27\pi$
Isotropic flux			$23{,}90\pi$

The region of gravitational capture of the nonrelativistic particles is situated far from the hole ($\rho\sim c/v_0$). In this region, the "Coriolis" acceleration due to rotation with the velocity (4.21) is for incidence parallel to the axis

$$\mathbf{w}_{\parallel}=\frac{4M^2a}{r^3}\frac{\rho_{\parallel}^2v_0^2}{r^2}\mathbf{e}^{\varphi}$$

and this leads to a twisting of the trajectory in the direction of rotation of the hole, while for incidence in the equatorial plane it is

$$\mathbf{w}_{\perp}=\frac{2M^2av_0}{r^3}\left(\frac{\rho_{\perp}}{r}\mathbf{e}^{r}+\mathbf{e}^{\varphi}\right)$$

and corresponds to the presence of an effective repulsion of a particle moving in the direction of the rotation, this repulsion increasing with decreasing initial velocity of the particle. Therefore, particles are more readily captured by the hole when incident parallel to the axis. The region of photon capture is situated much closer to the hole, in the strong-field region. The angular velocity acquired by a test body incident parallel to the axis is

$$\frac{d\varphi}{dt_{\parallel}}=\frac{2ar}{(r^2+a^2)^2}.$$

For incidence in the plane of the equator, it is

$$\frac{d\varphi}{dt_{\perp}}=\frac{\rho_{\perp}v_0(r-r_{\varphi})}{r(r^2+a^2)-2a(\rho_{\perp}v_0-a)},$$

where $r_{\varphi}=2[1-(a/\rho_{\perp}v_0)]$ is a turning point with respect to the angle φ. Since the photons in the equatorial plane are subject to a stronger twisting action on the part of the hole, they are more readily captured by the hole when incident perpendicular to the rotation axis.

5. INFALL TRAJECTORIES

The trajectories of particles and photons incident on a black hole with arbitrary initial angle ϑ_0 depend strongly on the projection of the orbital angular momentum of the particle onto the rotation axis. Nonrelativistic particles falling from infinity to a rotating black hole purely radially ($\rho_{\perp}=\rho_{\parallel}=L_z=Q=0$) arrive at a certain point $r\gg r_+$ at the time[39]

$$t\approx-\frac{4}{3}\left(\frac{r}{2}\right)^{3/2}-4\left(\frac{r}{2}\right)^{1/2}+\left[4+a^2\left(\frac{1}{2}-\sin^2\vartheta_0\right)\right]\left(\frac{2}{r}\right)^{1/2}.$$

The dependence on ϑ_0 revealed in the third term means that particles moving in the equatorial plane fall faster than particles moving along the symmetry axis. Therefore, in terms of the coordinate time t, i.e., from the point of view of a distant observer, a flux of particles that is spherical at infinity is drawn out, as it falls, along the symmetry axis, as shown in Fig. 8.[39]

For small projections of the orbital angular momentum of the particles, in the interval

$$0<L_z^2<a^2(E^2-1), \tag{5.1}$$

the region of variation of the polar angle ϑ and the nature of the trajectory is determined by the behavior of the latitude

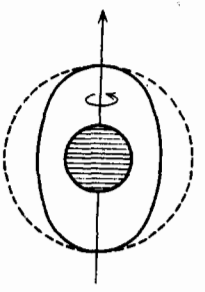

FIG. 8. Deformation of a spherical shell of particles that fall onto a rotating black hole.

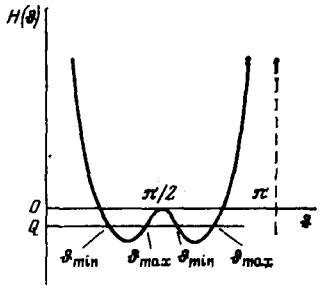

FIG. 9. Latitude potential $H(\vartheta)$ for $E^2>1$ and $L_z^2<a^2(E^2-1)$.

potential $H(\vartheta)$ which is shown in Fig. 9 (Ref. 14), for $E^2>1$. The admissible values of the polar angle of the incident particle are in the interval $\vartheta_{\min}<\vartheta<\vartheta_{\max}$, the range of variation of ϑ for $Q<0$ being restricted to one of the hemispheres.[14,61,62] i.e., the trajectory of the particle is situated between two hyperboloids $\vartheta=\vartheta_{\min}$ and $\vartheta=\vartheta_{\max}$. The condition of arriving on such a trajectory has in terms of the impact parameters the form[32]

$$\rho_\parallel^2+\rho_\perp^2\cos^2\vartheta_0<a^2\cos^2\varphi_0. \tag{5.2}$$

Analysis of Eqs. (3.1), (3.3), and (3.4) shows[32] that for geodesics of this type the radius r of the trajectory decreases monotonically; to reach the surface of the event horizon, the particle requires a finite proper time and an infinite time according to the clock of a distant observer, who measures the coordinate time t; the azimuthal angle φ increases monotonically for $\rho_\perp>0$; for $\rho_\perp<0$ it decreases far from the black hole but, beginning at distances

$$r<1-\frac{a\sin^2\vartheta}{v_0\rho_\perp\sin\vartheta_0}+\left[\left(1-\frac{a\sin^2\vartheta}{v_0\rho_\perp\sin\vartheta_0}\right)^2-a^2\cos^2\vartheta\right]^{1/2},$$

the angle φ then increases, i.e., as the hole is approached, all the trajectories wind in the direction of its rotation. In the limit $\vartheta_0\to\pi/2$, these quasiradial geodesics tend to equatorial geodesics with $\rho_\perp^2<a^2$. In the limit $a\to0$, all infall trajectories determined by the condition (5.2) go over into trajectories of radial falling.

The simplest quasiradial infall trajectories are the geodesics on which the value of the polar angle remains constant and equal to ϑ_0 during the motion. They are situated at the minima of the latitude potential $H(\vartheta)$ (Fig. 9). To them correspond the integrals of the motion

$$Q=-a^2(E^2-1)\cos^4\vartheta_0, \qquad L_z^2=a^2(E^2-1)\sin^4\vartheta_0$$

and the impact parameters $\rho_\perp=a\sin\vartheta_0$, $\rho_\parallel=0$. The infall trajectories with $\vartheta=\vartheta_0=\text{const}$ for $v_0<1$ can be expressed in terms of elliptic integrals,[5] and in the limit $v_0\to1$ are described explicitly by the formulas[32]

$$\left.\begin{aligned} r&=-Ev_0\tau \quad \text{for any value of } a\\ -tv_0&=r+\ln\Delta+\frac{1}{(1-a^2)^{1/2}}\ln\frac{r-1-(1-a^2)^{1/2}}{r-1+(1-a^2)^{1/2}},\\ \varphi&=\varphi_0+\frac{a}{2(1-a^2)^{1/2}}\ln\frac{r-1+(1-a^2)^{1/2}}{r-1-(1-a^2)^{1/2}} \end{aligned}\right\} a\neq1, \tag{5.3}$$

$$-tv_0=r+2\ln(r-1)-\frac{2}{r-1},$$

$$\varphi=\varphi_0+\frac{1}{r-1} \quad \text{for } a=1.$$

The photon geodesics of this class are physically distinguished trajectories in the Kerr metric. They are determined by the values

$$L_z=aE\sin^2\vartheta_0, \qquad Q=-a^2E^2\cos^4\vartheta_0$$

and form a special family, called a principal null congruence (a congruence is a family of lines that fill a space without intersecting or it is a ruled surface. The radial component of the wave vector of a photon of a principal null congruence is

$$k_r=-E. \tag{5.4}$$

In the Kerr metric, there are two principal null congruences. The second is characterized by the value

$$k_r=+E \tag{5.5}$$

of the radial component of the wave vector and describes outgoing photons whose world lines are null "generators" of the horizon—it is precisely these and only these photons that can remain forever on the horizon. Their angular velocity

$$\frac{d\varphi}{dt}=\frac{a}{r_+^2+a^2}$$

is equal to the rotation angular velocity (2.5) of the hole. The world lines of the photons of the principal null congruences are shown in the Kerr diagram (Fig. 10; Ref. 18) for the equatorial section of an extremal black hole. The world lines of the outgoing photons are represented in the form of broken spiral lines. The physical meaning of the principal null congruence (5.4) becomes clear when one goes over to Kerr coordinates, which are related to the Boyer-Lindquist coordinates by the transformation

$$d\tilde V=dt+\frac{r^2+a^2}{\Delta}dr, \qquad d\tilde\varphi=d\varphi+\frac{a}{\Delta}dr. \tag{5.6}$$

They are a generalization to the case of rotation of the Eddington-Finkelstein coordinates of the Schwarzschild metric and are formed by the world lines of freely falling photons: the "radial" geodesic of such a photon has the coordinates $(\tilde V,\vartheta,\tilde\varphi)=\text{const}$. The world lines of the photons of the principal null congruence directed inward form on the Kerr diagram the conical surface $\tilde V=\text{const}$. The coordinate $\tilde\varphi$ is an untwisted azimuthal coordinate, and therefore the diagram does not show a tilting of the light cones due

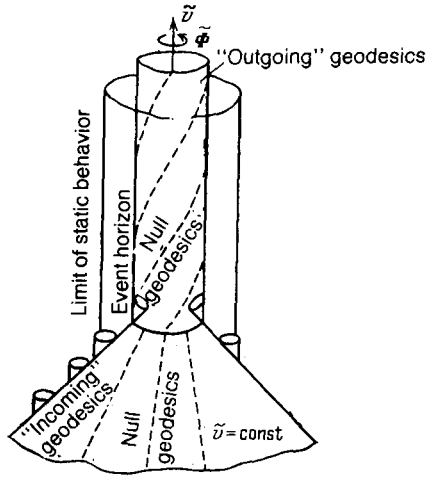

FIG. 10. Kerr diagram for equatorial section of an extremal black hole.

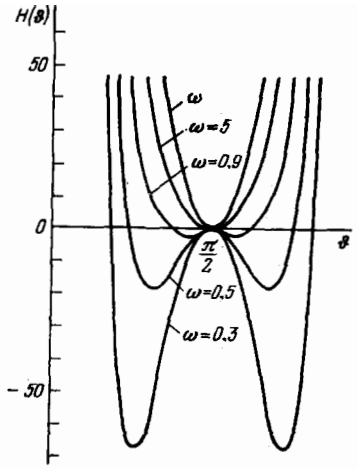

FIG. 11. Evolution of the latitude potential $H(\vartheta)$ with increasing ratio $L_z^2/a^2(E^2-1)$ (the largest is $\omega = 10$).

to dragging of the inertial frames in the direction of increasing $\tilde{\varphi}$, which occurs in the coordinates $(r, t, \vartheta, \varphi)$. On the event horizon, the light cones are completely tilted inward, except for the tangent line.

With increasing orbital angular momentum of the incident particles, there is a decreasing probability of their arriving on trajectories corresponding to the potential wells in the curve of the latitude potential $H(\vartheta)$. The behavior of the potential curves $H(\vartheta)$ with increasing value of

$$\omega = L_z^2 [a^2 (E^2 - 1)]^{-1} \tag{5.7}$$

is shown in Fig. 11 (Ref. 14). With increasing ω, the depth of the minima of the potential curves rapidly decreases. In the limit $\omega \to 1$, the minima are effectively smoothed, and at $\omega = 1$ there remains one minimum at $\vartheta = \pi/2$. In the case $\omega > 1$, the nature of the motion is determined by the potential curves shown in the upper half of Fig. 11. With increasing ω, these curves become narrower and narrower, i.e., the infall trajectories approach closer and closer to the equatorial plane.

The quasiradial geodesics $\vartheta = \text{const} = \vartheta_0$ are also physically distinguished for nonrelativistic particles. An ensemble of weakly interacting test particles incident on a rotating black hole is described in the first approximation by motion in a given potential under the action of a stochastic force, which can be taken to be a random Gaussian force δ-correlated with respect to the proper time.[9] The distribution of the probability of the resulting orbits with respect to the polar angle ϑ has the following remarkable properties[9]: 1) for $\omega \geqslant 1$, a maximum of the probability density is attained in the equatorial plane; 2) for $0 < \omega < 1$, the maximum of the probability density is split into two maxima, to which correspond values of the polar angle

$$\vartheta_{1,2} = \pm \sin^{-1} \omega^{1/4},$$

characterizing the positions of the minima of the curve $H(\vartheta)$ (see Fig. 9), i.e., the orbits of the particles tend to collect on the surfaces $\vartheta_1 = \text{const}$ and $\vartheta_2 = \text{const}$.

6. BOUND STATES

6.1. Spherical orbits

The simplest and best studied case of bound motion corresponds to the spherical ($r = \text{const}$) orbits.[95,67,12] Stable spherical orbits of photons can exist only below the inner ($r = 1 - (1-a^2)^{1/2}$, $\Delta(r_-) = 0$) event horizon,[89] but, because of the instability inherent in the interior region of a rotating black hole, these orbits evidently have only a formal meaning. The spherical orbits of particles (timelike bound geodesics) are determined by simultaneous solution of the equations

$$R(r_0) = 0 \qquad \text{(spherical orbit)}, \tag{6.1}$$

$$\left.\frac{\partial R}{\partial r}\right|_{r_0} = 0 \qquad \text{(extremum of potential, guaranteeing preservation of the condition } r_0 = \text{const}), \tag{6.2}$$

$$\left.\frac{\partial^2 R}{\partial r^2}\right|_{r_0} > 0 \qquad \text{(condition of stability)}. \tag{6.3}$$

Reversal of the sign in (6.3) determines the family of unstable spherical orbits. Equations (6.1)–(6.3) are augmented by the condition of bound motion, $Q \geqslant 0$, and then the values of r_0, E, L_z, and Q are completely determined. The family of stable spherical orbits in the neighborhood of an extremal Kerr hole is shown in Fig. 12 (Ref. 95) in the form of a two-dimensional surface in the (r, L_z, Q) space. The intersections of this surface with the plane $Q = 0$ represent the circular orbits in the plane of the equator. For orbit radii $r_0 \geqslant 9$ there are two lines of intersection, corresponding to direct and retrograde orbits. The nature of the orbit is determined by the sign of the projection of the orbital angular momentum onto the rotation axis L_z. Direct stable circular orbits in the equatorial plane exist up to $r = r_+$. The retrograde circular orbits become unstable once the orbit radius reaches $r_0 = 9$.

For fixed radius of the orbit, the energy in the orbit varies monotonically along the surface shown in Fig. 12. The direct circular equatorial orbits have the greatest binding energy $W = 1 - E$, and the retrograde orbits for $r_0 \geqslant 9$ the

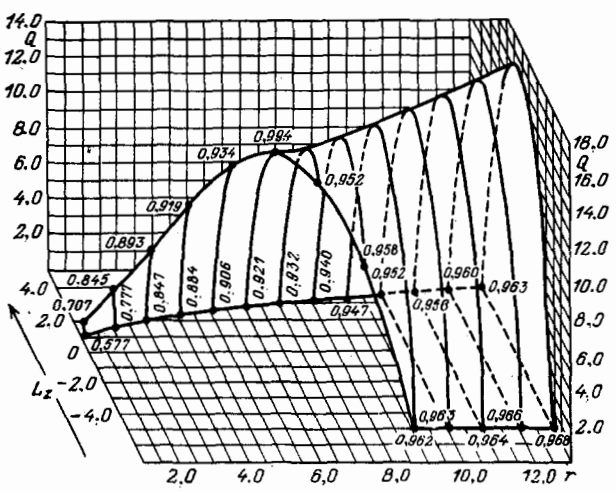

FIG. 12. Part of the surface of spherical orbits in the field of an extremal black hole.

lowest binding energy. For $r_0 < 9$, the lowest binding energy corresponds to orbits transitional from the stable to the unstable ones and situated at the points of inflection of the radial potential, where $\partial^2 R/\partial r^2 = 0$. These orbits represent the edge of an opening in the surface under consideration. The binding energy characterizes the energy that can be emitted in the form of gravitational waves by a body falling toward a black hole with initial energy $E \gtrsim 1$ when it is captured by the corresponding orbit.

In the general case of nonequatorial motion, a spherical orbit is said to be direct if the displacement $\Delta\varphi$ of the particle's azimuth in the orbit during the time of one cycle in latitude is positive. The azimuthal displacement per cycle is determined by the expression[95]

$$\Delta\varphi = \frac{4}{[z_+(1-E^2)]^{1/2}}\left\{L_z \Pi\left(-z_-, \left(\frac{z_-}{z_+}\right)^{1/2}\right) + \left[\frac{E(r^2+a^2)-aL_z}{\Delta} - E\right] K\left(\frac{z_-}{z_+}\right)^{1/2}\right\}; \tag{6.4}$$

here, $z = \cos^2\vartheta$ and z_- and z_+ are turning points with respect to the angle ϑ (roots of Eq. (3.2)); Π and K are elliptic integrals of the first and second kind. The first term on the right-hand side has the sign of L_z, while the second is always positive for spherical orbits that satisfy the condition (3.12a). For negative values of L_z, the first term always remains predominant, since with decreasing L_z the integral $\Pi(-z_-, (z_-/z_+)^{1/2})$ increases sharply.

Stable spherical direct orbits exist until the surface of the event horizon is reached. The one-parameter family of orbits that "slip" along the horizon is characterized by a value of L_z in the interval

$$\frac{2}{\sqrt{3}} \leqslant L_z \leqslant 2 \qquad (a=1). \tag{6.5}$$

The lower limit is obtained from the condition of a bound motion, $Q \geqslant 0$, and the upper from the stability condition (6.3). The values of the integrals of the motion Q and E can be uniquely expressed in terms of L_z:

$$E = \frac{L_z}{2}, \qquad Q = \frac{3}{4}L_z^2 - 1. \tag{6.6}$$

The limiting direct spherical orbits are shown in Fig. 13 (Ref. 95). The particle moves along a spiral lying on the surface of a sphere between the lines of maximal and minimum latitude, which are situated symmetrically on the two sides of the equator. The values of the limiting polar angle $|\vartheta_{\max}|$ vary from 0° for an orbit with $L_z = 2/\sqrt{3}$, lying in the equatorial plane, to 25° for a spherical orbit with $L_z = \sqrt{2}$,

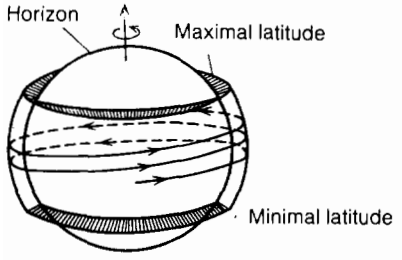

FIG. 13. Limiting spherical orbits in the field of an extremal black hole.

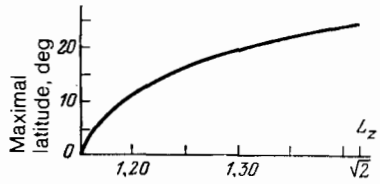

FIG. 14. Dependence of maximal latitude of limiting spherical orbits on the angular momentum in the orbit.

$E = 1/\sqrt{2}$, and $Q = 1/2$. The dependence of $|\vartheta_{\max}|$ on L_z is shown in Fig. 14.[95]

The line of intersection of the surface of the spherical orbits with the plane $L_z = 0$ determines polar circular orbits passing alternately over the north and south poles. Stable polar orbits exist for values $Q > a^2(1 - E^2)$ down to the minimal radius $r_{0\min}$, which is determined by the condition[16]

$$2E^2 r(r^2 + a^2) - E^2(r-1)(r^2+a^2)\Delta^{-1} - r\Delta = 0$$

and the condition (6.3). For an extremally rotating black hole, $r_{0\min} = 2.53$. The minimal radius of an unstable circular polar orbit satisfies the equation

$$r_{\rm ph}^3 - 3r_{\rm ph}^2 + a^2 r_{\rm ph} + a^2 = 0.$$

As $r \to r_{\rm ph}$, the energy on the orbit increases without limit, i.e., the limiting unstable polar orbit is a photon orbit. Its radius lies in the interval from $r_0 = 3$ for $a = 0$ to $r_0 = 1 + \sqrt{2}$ for $a = 1$.

6.2. Circular equatorial orbits

These orbits, which are of special astrophysical interest, for example, for the study of processes of disk accretion, have been investigated most fully in the Kerr metric (Refs. 34, 35, 42, 60, 71, and 84). The effective radial potential $U_\pm(r)$ in the plane of the equator has the form[34]

$$U_+ = \frac{\Delta^{1/2}\{r^2L_z^2 + [r(r^2+a^2)+2a^2]r\}^{1/2} + 2aL_z}{r(r^2+a^2)+2a^2}. \tag{6.7}$$

The stable circular orbits are situated at the minimum of the curve $U_+(r)$, the unstable orbits at the maximum. For null (photon) orbits, Eq. (6.7) is reduced to the form

$$U_\pm = \pm\frac{L_z(r\Delta^{1/2} \pm 2a)}{r(r^2+a^2)+2a^2},$$

from which it follows that all the circular equatorial photon orbits are unstable—the effective potential $U_+(r)$ for the photons has in the region $r_+ \leqslant r < \infty$ only a maximum; all null geodesics have at most a single turning point and, therefore, are unstable for both signs of L_z.

The simultaneous solution of the equations $R = 0$ and $\partial R/\partial r = 0$ for E and L_z gives the integrals of the motion as functions of the orbit radius[34,35]:

$$E = \frac{r^{3/2} - 2r^{1/2} \pm a}{r^{3/4}(r^{3/2} - 3r^{1/2} \pm 2a)^{1/2}}, \tag{6.8}$$

$$L_z = \frac{r^2 \mp 2ar^{1/2} + a^2}{r^{3/4}(r^{3/2} - 3r^{1/2} \pm 2a)^{1/2}}.$$

The upper sign corresponds to direct orbits, the lower to retrograde. From the point of view of a distant observer, the angular velocity in the orbit is

$$\frac{d\varphi}{dt} = \pm\frac{1}{r^{3/2} \pm a}. \tag{6.9}$$

TABLE II. Limiting stable circular orbits in the gravitational field of a massive body (black hole).

	Newtonian orbits	Schwarzschild orbits	Kerr orbits ($a=1$)	
r_0	0	6	1	9
E	$-\infty$	$\frac{2\sqrt{2}}{3}$	$\frac{1}{\sqrt{3}}$	$\frac{5}{3\sqrt{3}}$
$W=1-E$	$+\infty$	5.72%	42.35%	3,77%
L_z	0	$2\sqrt{3}$	$\frac{2}{\sqrt{3}}$	$-\frac{22}{3\sqrt{3}}$

while the physical rotation velocity is

$$v_\varphi = \pm \frac{r^2 \mp 2ar^{1/2}+a^2}{\Delta^{1/2}(r^{3/2}\pm a)}.$$

At large distances from the center, the binding energies of the direct and retrograde orbits are almost equal. With decreasing r, the spin-orbit interaction becomes stronger, and this increases the binding energy of the direct orbits and decreases the binding energy of the retrograde orbits compared with the Schwarzschild orbits. The maximal binding energy and the minimal value of the angular momentum correspond to the limiting stable orbit, the radius of which can be determined from the equations[34]

$$\left.\begin{aligned} r_{ms} &= 3+z_2 \mp [(3-z_1)(3+z_1+2z_2)]^{1/2}, \\ z_1 &= 1+(1-a^2)^{1/3}[(1+a)^{1/3}+(1-a)^{1/3}], \\ z_2 &= (3a^2+z_1^2)^{1/2}. \end{aligned}\right\} \quad (6.10)$$

The parameters of the limiting circular orbits in the equatorial plane of an extremally rotating black hole are given in Table II,[84] where they are compared with the corresponding characteristics for the Newtonian and Schwarzschild cases.

With a further decrease in the radius of the unstable orbits, the value of E determined from Eq. (6.7) becomes greater than unity once a certain radius r_{mb} of the orbit is reached, and the orbits then become unbound. The radius of the limiting bound orbit is the minimal pericenter of a parabolic ($E\approx 1$) orbit[35]:

$$r_{mb} = 2 \mp a + 2(1 \mp a)^{1/2}.$$

With further tending of r to r_+, there comes a moment at which the denominator of the expression (6.8) vanishes and the values of E and L_z become infinitely large. Here there is the limiting unstable photon orbit, whose radius

$$r_{ph} = 2\left\{1+\cos\left[\frac{2}{3}\cos^{-1}(\mp a)\right]\right\}$$

corresponds to impact parameter value

$$\frac{L_z}{E} = \pm \frac{1}{2} r_{ph}^{1/2}(r_{ph}+3).$$

Figure 15 (Ref. 35) shows how the radii of the limiting stable orbit (r_{ms}), the limiting bound innermost orbit (r_{mb}), and the limiting photon orbit (r_{ph}) in the equatorial plane of the black hole depend on their specific angular momentum. The continuous curve is the dependence of the radius r_+ of the event horizon on a. The straight line r_m is the equatorial boundary of the ergosphere. From the point of view of a distant observer measuring the radial coordinate r, the radii of the three direct limiting orbits coincide in the limit $a\to 1$ with the radius of the event horizon $r_+\to 1$. This coincidence occurs because an infinitesimally small change of the radial coordinate r corresponds in the limit $r\to r_+$ to an infinitely large change of the radial distance R. In accordance with (2.1) or (1.1),

$$R = \int \frac{r}{\Delta^{1/2}}\,dr \to r + \ln(r-1) \quad \text{as} \quad a\to 1.$$

If the specific angular momentum a differs very little from unity, $a = 1-\varepsilon$, $\varepsilon \ll 1$, then[35]

$$r_+ \approx 1+(2\varepsilon)^{1/2},\ r_{ph} \approx 1+2\left(\frac{2\varepsilon}{3}\right)^{1/2},$$

$$r_{mb} \approx 1+2\varepsilon^{1/3},\quad r_{ms} \approx 1+(4\varepsilon)^{1/3},$$

and the radial distances between the limiting orbits and the horizon are

$$R_{+ph} \approx \frac{1}{2}\ln 3,\quad R_{+mb} \approx \ln(1+\sqrt{2}),$$

$$R_{+ms} \approx \ln(2^{7/6}\varepsilon^{-1/6}) \to \infty.$$

At the same time,

$$E \to \frac{1}{\sqrt{3}},\quad v_\varphi \to \frac{1}{2} \quad \text{for} \quad r\to r_{ms},$$

$$E = 1,\quad v_\varphi \to \frac{1}{\sqrt{2}} \quad \text{for} \quad r\to r_{mb}.$$

It is interesting to note that the angular velocity v_φ on the orbit $r = r_{ms}$ in the case $a = 1$ is the same as in the case $a = 0$, despite the fact that for $a = 1$ the orbit is in a stronger gravitational field. This circumstance, like the lagging of Mercury's perihelion associated with rotation, is due to the dragging of the inertial frames.

6.3. Influence of frame dragging effect on orbital motion

The classical results describing the influence of the rotation of a source on the orbital motion in the weak-field

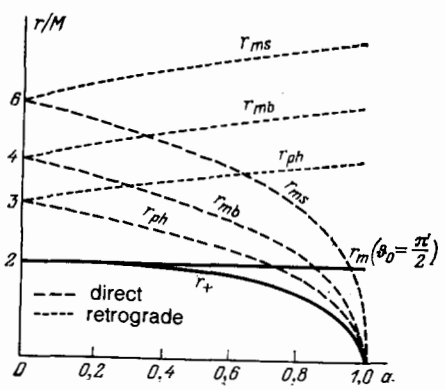

FIG. 15. Limiting circular orbits in the equatorial plane.

approximation are due to Lense and Thirring.[73] They showed that for noncircular orbits in the plane of the equator the dragging of the inertial frames by the gravitational field of a rotating body leads to an additional displacement of the periastron of the orbit: in each revolution in the orbit, the azimuthal angle φ changes by the amount[66,73]

$$\Delta\varphi = 2\pi\left(1+\frac{3}{L_z^2}-\frac{4a}{L_z^3}\right). \tag{6.11}$$

The influence of rotation on spherical orbits reduces to a dragging of their nodes (the points of intersection of the orbits with the equatorial plane) in the direction of rotation of the central body. In the weak-field approximation, a node is displaced after each revolution in the orbit through the following angle in the direction of the rotation:

$$\Delta\Omega = \frac{2a}{r_0^{3/2}}. \tag{6.12}$$

In the general case, the value of $\Delta\Omega$ depends on the ratio of the frequencies of the oscillations in the latitude, ν_ϑ, and azimuthal, ν_φ, directions. If these frequencies were equal, then during one cycle in latitude the angle φ would change by 2π. Therefore, the ratio of the frequencies has in the general case the form

$$\frac{\nu_\varphi}{\nu_\vartheta} = \frac{\Delta\varphi}{2\pi}. \tag{6.13}$$

As numerical calculations show,[95]

$$\begin{aligned} &\frac{\nu_\varphi}{\nu_\vartheta} < 1 \quad \text{for} \quad L_z < 0, \\ &\frac{\nu_\varphi}{\nu_\vartheta} > 1 \quad \text{for} \quad L_z > 0, \end{aligned} \tag{6.14}$$

i.e., the nodes of spherical orbits are always dragged in the direction of the rotation. The angle of drag in one revolution is

$$\Delta\Omega = 2\pi\left|\frac{\nu_\varphi}{\nu_\vartheta}-1\right|. \tag{6.15}$$

The dependence of $\Delta\Omega$ on the orbit radius for the case $a = 1$ is shown in Fig. 16 (Ref. 95). For $r_0 \gg r_+$, the angle $\Delta\Omega$ decreases as $r^{-3/2}$, in accordance with the Lense-Thirring formula. In the limit $r_0 \to r_+$, the angle $\Delta\Omega$ increases in accordance with the law

$$\Delta\Omega = \frac{2\pi\alpha}{r_0 - r_+}, \tag{6.16}$$

where the numerical coefficient α varies in the range from 0.817 to 0.835 for variation of the angular momentum in the orbit in the interval (6.5). In the strong-field region, the angle $\Delta\Omega$ of dragging depends not only on the orbit radius, as in the Lense-Thirring approximation, but also on the value of L_z (spin-orbit interaction). For example, for orbits with radius $r_0 = 9$ near the equatorial plane, the value of $\Delta\Omega/(2\pi)$ varies from 0.0814 for an orbit with $L_z < 0$ to 0.0607 for an orbit with $L_z > 0$.

The displacement of the periastron of noncircular equatorial orbits was obtained[13] in a more general case in analytic form to terms of order $(M/r)^3$. In terms of the focal parameter p and the orbit eccentricity e, which are related to E and L_z by

$$\begin{aligned} E^2 &= 1-\frac{M(1-e^2)}{p}+\frac{(1-e^2)^2M^2}{p^2}, \\ L_z^2 &= Mp\left[1+\frac{M(3+e^2)}{p}-\frac{2M^{3/2}a(3+e^2)}{p^{3/2}}\right], \end{aligned} \tag{6.17}$$

the displacement of the orbit periastron is determined by

$$\begin{aligned} \frac{\Delta\varphi}{\pi} &= \frac{3M}{p}-\frac{4M^{3/2}a}{p^{3/2}}\left(1+\frac{9M}{p}\right) \\ &+\frac{3M^2}{2p^2}\left(9+a^2+\frac{e^2}{2}\right) \\ &+\frac{3M^3}{2p^3}\left(45+25a^2-3a^2e^2+\frac{15e^2}{2}\right). \end{aligned} \tag{6.18}$$

In the strong-field region, the displacement of the periastron has been calculated numerically for individual orbits.[67,96] It follows from the calculations that the additional displacement $\Delta\varphi$ due to rotation increases with increasing energy of the particle in the orbit. An example of a noncircular equatorial orbit is given in Fig. 17 (Ref. 67). For positive L_z, the orbit consists of two geometrically distinct parts: an elliptic part and a spiral part. Beginning at the apoastron, the particle moves along the elliptic part of the orbit; then, near the horizon it makes several turns around the center along the spiral section, reaches the periastron, and returns again to the elliptical section, where it reaches the next point of apoastron. The closer E is to the energy $E_{\max}$ in the first unstable orbit, the greater is the number of turns in the spiral section. In the limit $E_{\max} - E \to 0$, the particle reaches at the periastron an unstable orbit, where it can, in principle, remain for an arbitrarily long time. For orbits with negative L_z, the spiral section is much more pronounced.

In the general case of nonequatorial and nonspherical orbits, numerical calculation of a motion of a cloud of parti-

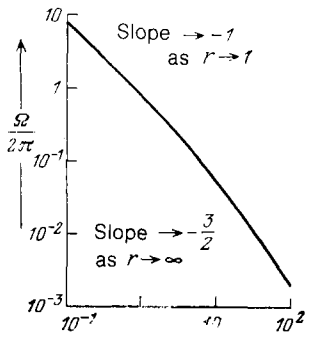

FIG. 16. Dragging of nodes of spherical orbits in the field of a rotating black hole.

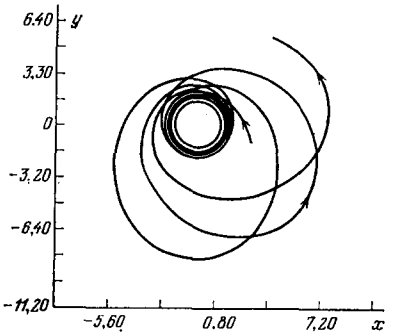

FIG. 17. Noncircular equatorial orbit in the plane of an extremal black hole. $L_z = 2$, $E = 0.9$, number of turns along the spiral section $n = 3$.

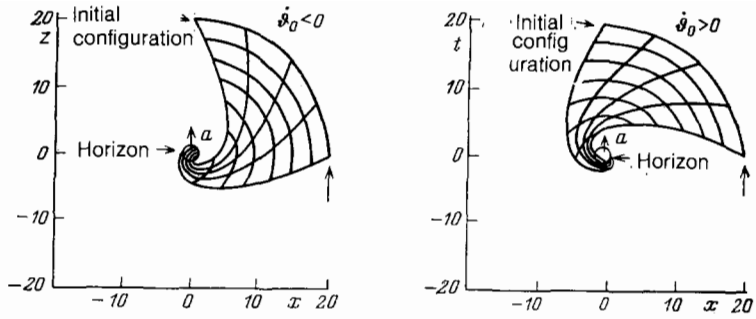

FIG. 18. Motion of a cloud of particles with $E = 1$, $L_z = 0$, and $Q = 10$ in the field of an extremal black hole.

cles with energies $E = 1$ ($L_z = 0$) in the neighborhood of an extremal black hole (Fig. 18; Ref. 96) shows that all the particles in the cloud that initially had zero angular momentum L_z ultimately acquire an angular velocity equal to that of the hole.[96]

The effect of the dragging is manifested not only in the different deformations of the orbits described above. The difference between the revolution periods of two test bodies in the same circular equatorial orbit moving in opposite directions leads to relativistic drift of the point of encounter of these bodies. This effect, called by the authors[19] the planetary gravitational Zeeman effect, depends neither on the radius of the orbit nor on the mass of the central body, nor even on the gravitational constant, but only on the specific angular momentum of the gravitating body. In accordance with (6.9), the period of revolution of a test body in a circular equatorial orbit is

$$T_{\pm} = 2\pi (r_0^{3/2} \pm a) = T_N + \Delta T. \tag{6.19}$$

The first term also follows from Newton's theory, while the second represents the relativistic correction, which depends only on a. The condition of meeting of two bodies moving in circular equatorial orbits of the same radius in opposite directions has the form

$$\Delta t\,(\dot{\varphi}_+ - \dot{\varphi}_-) = 2\pi n, \qquad n = 0,\ 2,\ 4,\ \ldots\ .$$

The drift of the place of meeting during one revolution is

$$\delta = \frac{4\pi\dot{\varphi}_+}{\dot{\varphi}_+ - \dot{\varphi}_-} - 2\pi = \frac{2\pi(\dot{\varphi}_+ + \dot{\varphi}_-)}{\dot{\varphi}_+ - \dot{\varphi}_-}.$$

The effective drift per unit time (in radians) is determined as

$$\left|\frac{\delta}{T_N}\right| \approx \frac{\dot{\varphi}_+ + \dot{\varphi}_-}{2}$$

and is 4".4/100 yr for the Earth, 280"/100 yr for Jupiter, and 600"/100 yr for the Sun.[19]

7. BENDING OF LIGHT RAYS

The equations describing the propagation of radiation in the gravitational field of a rotating body, provided that the wavelength is much less than the characteristic scale of variation of the field, are obtained by integrating Eqs. (3.1)–(3.4) and have the form (see, for example, Ref. 18)

$$\int \frac{d\vartheta}{[Q - H(\vartheta)]^{1/2}} = \int \frac{dr}{[R(r)]^{1/2}}, \tag{7.1}$$

$$\varphi = -\int \frac{aE\sin^2\vartheta - L_z}{\sin^2\vartheta\,[Q - H(\vartheta)]^{1/2}}\,d\vartheta + a\int \frac{E(r^2+a^2) - aL_z}{\Delta\,[R(r)]^{1/2}}\,dr, \tag{7.2}$$

$$t = -a\int \frac{aE\sin^2\vartheta - L_z}{[Q - H(\vartheta)]^{1/2}}\,d\vartheta + \int \frac{(r^2+a^2)[E(r^2+a^2) - aL_z]}{\Delta\,[R(r)]^{1/2}}\,dr. \tag{7.3}$$

The azimuthal deflection of a ray coming from infinity in the equatorial plane is determined by the expression

$$\Delta\varphi = -2\int_{\infty}^{d} \frac{\rho_\perp r^2 - 2r(\rho_\perp - a)}{\Delta\,[r^4 - r^2(\rho_\perp^2 - a^2) + 2r(\rho_\perp - a)]^{1/2}}\,dr, \tag{7.4}$$

where the letter d denotes the dimensionless distance of closest approach of the photon and the deflecting body.

In the weak-field approximation ($d \gg r_+$), the deflection of the ray in the equatorial plane can be obtained from (7.4) in the explicit form

$$\Delta\varphi = \frac{4}{d} + \frac{15\pi - 16}{4d^2} - \frac{4a}{d^2}\,\frac{\rho_\perp}{|\rho_\perp|}. \tag{7.5}$$

The first term describes the famous bending of light rays in the gravitational field of a massive body predicted by Einstein, in magnitude $\delta\varphi = 1".75$ for a ray grazing the edge of the Sun. The correction that depends on the rotation[7,27,42,79] has opposite signs depending on the motion of the photon—in the direction of the rotation or in the opposite direction. As a result, rays with negative impact parameters are deflected more strongly than rays with positive ones (see Fig. 6). Combining the expressions for $\Delta\varphi$ for the two rays with impact parameters equal in magnitude but opposite in sign, one can in principle determine the angular momentum of the deflecting body.

The latitude deflection and the azimuthal twisting of a ray propagating parallel to the rotation axis are described by[7,27]

$$\Delta\vartheta = \pi + \frac{4}{\rho_{\parallel}} + \frac{15\pi}{4\rho_{\parallel}^2}, \quad \Delta\varphi = \frac{4a}{\rho_{\parallel}^2}. \tag{7.6}$$

In the case of an arbitrarily oriented ray trajectory, the ray is characterized by three parameters (Fig. 19): the radius d of closest approach, the value of the coordinate ϑ at $r = d(\vartheta_d)$, and the angle η_d between the tangent to the spatial trajectory and the Killing vector ξ_φ. The constants of the motion and the extremal value of the coordinate ϑ, equal to ϑ_e, can be expressed in terms of these three parameters[20]:

$$\sin\vartheta_e = \sin\vartheta_d\cos\eta_d\left(1 - \frac{2a}{d}\,\frac{\sin\vartheta_d\cdot\sin^2\eta_d}{\cos\eta_d}\right).$$

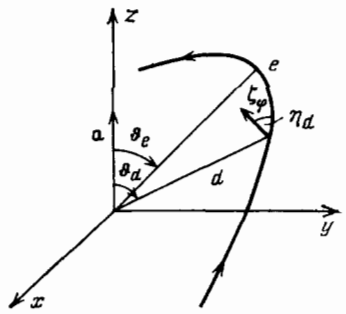

FIG. 19. Bending of a ray in the general case; η_d is the angle between the tangent to the spatial trajectory and the Killing vector ζ_φ; ϑ_e is the extremal value of the polar angle ϑ.

In the general case, the total deflection of the ray is given by[20]

$$\delta\Phi = \frac{4}{d}\left(1 + \frac{15\pi - 16}{16d} - \frac{\mathbf{ae}}{d}\right), \tag{7.7}$$

where **e** is a unit vector perpendicular to the plane of the orbit.

The azimuthal deflection of a ray passing in the equatorial plane in the immediate vicinity of the capture region is characterized by a logarithmic dependence of $\Delta\varphi$ on $\delta = d - r_0 \ll 1$:

$$\Delta\varphi = \frac{2a}{3-d}\left[A^\varphi\left(-\ln\delta + \ln\frac{3d}{1+(\sqrt{3}/2)}\right) + \sum_{r_-,\, r_+}\frac{B^\varphi_\pm}{[r_\pm(2d+r_\pm)]^{1/2}}\ln\frac{d\{[3r_\pm(2d+r_\pm)]^{1/2}+2r_\pm+d\}}{(d-r_\pm)\{[r_\pm(2d+r_\pm)]^{1/2}+r_\pm+d\}}\right], \tag{7.8}$$

where A^φ and B^φ are equal to

$$A^\varphi = \frac{d^2(d-1)}{\sqrt{3}\,d\Delta(d)},$$

$$B^\varphi_\pm = \frac{1}{2\Delta(d)}\left[a^2(3+d) - 2d(3-d) \pm \frac{a^2(3+d^2)-2d(3-d)}{(1-a^2)^{1/2}}\right]. \tag{7.9}$$

The effects of rotation are most pronounced in the case of an extremal black hole, for which a photon that arrives with positive impact parameter must be captured directly at the point $r_0 = r_+$. In the case of exact equality $a = 1$, the azimuthal deflection of a ray passing near the region of capture is proportional to $1/\delta$. Astrophysical rotating black holes most probably have specific angular momentum slightly different from unity $a = 0.998$ (see, for example, Refs. 29 and 33). The slight difference between a and unity leads to a qualitative change of the asymptotic behavior of the azimuthal deflection $\Delta\varphi$ near r_0, since when $a \to 1$ the point $r_0 \to r_+ = r_-$. Therefore, the azimuthal deflection of the ray in the limit $d \to r_0 \to r_+$ can be described in terms of the two small parameters ε and δ:

$$\Delta\varphi = \frac{4a}{3\sqrt{3}}\left(-\ln\delta + \ln\frac{3}{1+(\sqrt{3}/2)}\right) + \frac{a}{2\sqrt{3}\,[2\delta + (\varepsilon/6)^{1/2}]} \times \sum_{-\sqrt{3},\,+\sqrt{3}} \ln\left[1 + (2 \pm \sqrt{3})\,\frac{(2\varepsilon/3)^{1/2}}{\delta}\right] \times\left[1 + \frac{1 \pm 4\sqrt{3}}{2}\,\frac{\delta}{(2\varepsilon/3)^{1/2}}\right]. \tag{7.10}$$

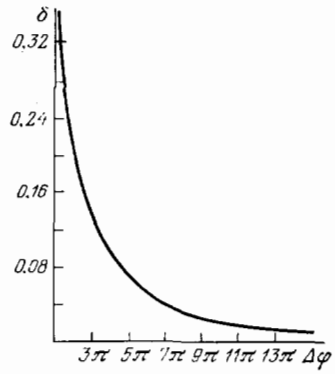

FIG. 20. Dependence of the deflection angle for photons passing near the capture region in the equatorial plane of an extremal black hole on the value of $\delta = d - r_+$.

The dependence of $\Delta\varphi$ on δ for $a = 0.998$ is shown in Fig. 20. For rays with negative impact parameters ($r_0 = 4$ for $d = 1$) $\Delta\varphi$ depends near the capture region logarithmically on δ:

$$\Delta\varphi = \frac{8}{3\sqrt{3}}\ln\delta - \frac{8}{3\sqrt{3}}\ln 12 + \left(\frac{8}{3\sqrt{3}} - \frac{10}{9}\right)\ln\left(1 + \frac{\sqrt{3}}{2}\right). \tag{7.11}$$

The rays close to the capture region, deflected by the hole through angles

$$\Delta\varphi \approx \pm 3k\pi, \qquad k = 1, 2, 3, \ldots, \tag{7.12}$$

form an "apparent edge of the hole" in the situation in which the hole is on the line of sight between the observer and the radiation source. The shape of the boundary of the luminous halo surrounding the image of the hole in the plane perpendicular to the line to the radiation source depends strongly on the angle between the line of sight and the rotation axis of the hole, since with increasing angle the shape of the photon scattering cross section becomes more and more asymmetric with respect to the center (see Fig. 7).

8. GRAVITATIONAL TIME DELAY OF SIGNALS

Until comparatively recently, there were three classical effects that tested the general theory of relativity: the displacement of Mercury's perihelion, the deflection of light in the gravitational field of a massive body, and the gravitational red shift. In 1964, Shapiro proposed a fourth test, which consisted of measuring the time needed for a signal sent from the Earth to reach some inner planet, be reflected from it, and return to the Earth (see Ref. 2 and the references given there). As the experiments of Shapiro's group showed, the gravitational time delay of a signal reflected by Mercury in the field of the Sun is 240 μsec, the accuracy of the measurements being $1.5 \cdot 10^{-6}$ sec.

Theoretically, the time of propagation of a signal, measured by a distant (from the gravitating body) observer is obtained by integrating along the complete propagation trajectory with allowance for the change in the gravitational field from point to point. In the equatorial plane of the rotating body, the time of propagation of the signal from the point R to the point of closest approach d, obtained by integrating

(7.3), has in the weak-field approximation ($d \gg r_+$) the form[7,8,13]

$$t_\perp = (R^2 - d^2)^{1/2} + 2\ln\frac{R+(R^2-d^2)^{1/2}}{d} + \left(\frac{R-d}{R+d}\right)^{1/2} + \frac{15\pi-8}{4d} - \frac{4a}{d}\frac{\rho_\perp}{|\rho_\perp|} \quad (8.1)$$

($R \gg d$).

The principal term corresponds to the signal propagation in flat space, and the second and third describe the gravitational time delay measured in Shapiro's experiments. The additional correction to the gravitational time delay of a radar signal due to the rotation of the Sun is characterized by the value $2.1\cdot10^{-10}$ sec,[13] which is as yet below the accuracy of the measurements.

However, allowance for the influence of rotation on the signal propagation time is in principle important physically, since the additional gravitational time delay in the gravitational field of the rotating body may be not only a delay but also an acceleration. For signals propagating in the equatorial plane, the sign of the additional delay due to the rotation depends on the direction of the signal—with or against the rotation. The propagation time of a signal traveling parallel to the rotation axis,[7,8]

$$t_\parallel = (R^2 - d^2)^{1/2} + 2\ln\frac{R+(R^2-d^2)^{1/2}}{d} + \left(\frac{R-d}{R+d}\right)^{1/2} + \frac{15\pi-8}{4d} + \frac{120-23\pi-4a^2}{4d^2} \quad (8.2)$$

($R \gg d \gg r_+$)

depends on the rotation to a higher order in the small ratio r_+/d than is the case for (8.1); moreover, the additional gravitational delay due to the rotation is negative. The quadratic dependence of $t_\parallel$ on a/d is in a certain sense analogous to the transverse Doppler effect of the special theory of relativity and means that for propagation of radiation parallel to the axis the frame dragging effect is not so important as in the equatorial plane, though the additional gravitational delay is an acceleration.

A photon incident on a rotating black hole from a certain point R along a quasiradial trajectory (5.3) has a positive value of the projection $L_z = aE\sin^2\vartheta_0$ of the angular momentum onto the axis. To reach the event horizon, it requires the time[32]

$$t = \left[r + \ln(r^2-2r) + \ln\left(1+\frac{a^2}{r^2-2r}\right) + \frac{1}{(1-a^2)^{1/2}}\ln\frac{r-1-(1-a^2)^{1/2}}{r-1+(1-a^2)^{1/2}}\right]\Bigg|_R^{r_+}, \quad (8.3)$$

which is less than the time of falling of a photon into a nonrotating black hole, which is determined by the first two terms in (8.3).

Thus, the influence of the dragging of the inertial fields by the gravitational field of the rotating body has the consequence that the additional "rotational" gravitational time delay may be not only a delay but also an acceleration. The signal propagation time in the gravitational field of a rotating body depends strongly on the orientation of the signal propagation direction relative to the rotation axis. This dependence is enhanced for signals propagating in the immediate vicinity of the region of gravitational capture of a rotating black hole. The analytic expressions describing in this case the signal propagation time are rather cumbersome,[7] but qualitatively the behavior of Δt as a function of δ and as a function of the sign of the impact parameter is similar to the behavior of the azimuthal deflection $\Delta\varphi$ (see the previous section). The difference between the propagation times of photons traveling in the equatorial plane of a rotating black hole near the capture region on different sides of the hole is shown in Fig. 21 (Ref. 7). For the deflection angles (7.13), it describes a relative gravitational time delay of signals traveling in the region in which the "apparent edge of the hole" (see Fig. 7) intersects the equatorial plane, i.e., the maximal relative time delay of the photons forming the luminous halo that is the boundary of the hole in the image of the radiation source illuminating it.

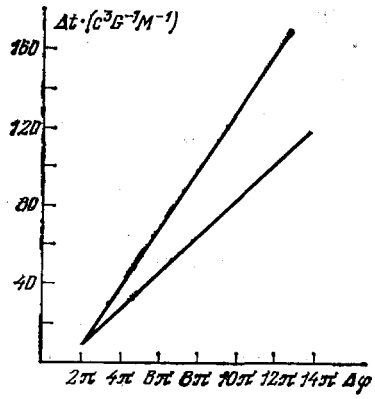

FIG. 21. Relative time delay of photons traveling in the equatorial plane of an extremal black hole on different sides of the axis (the lower curve is for Δt_{geom}, which is the purely geometrical time delay due solely to the geometrical path difference).

9. ROTATING GRAVITATIONAL LENS

The gravitational lens effect, predicted by Einstein in 1936, has recently acquired practical topicality. Several[3)] astrophysical objects are now known—double and triple quasars—that are interpreted as images of the same object formed by gravitational lenses lying on the line of sight between the quasars and the observer.[20,22,92–94] The gravitational lenses could be stars, galaxies, clusters of galaxies, and also black holes.

In the rigorous sense of the word, gravitational lenses are extended objects in which the matter distribution (and, thus, the refractive index) depends on the coordinates, although a focusing effect also occurs for a point gravitating mass; indeed, it was for such a case that it was first predicted (see Ref. 22 and the references given there). There is an extensive literature on gravitational lenses. The present section will be devoted to a single aspect of the theory of gravitational lenses—the possible consequences of rotation of the massive body that plays the part of the lens (Refs. 3, 7, 8, 20, 21, and 72), which are obtained for point lenses but evidently have a general nature. They are as follows.

First, it has been established that there is a displacement of the focus of a rotating lens compared with a nonrotating

lens[3,21]; in the first approximation, the focus of the Kerr lens is displaced relative to the axis passing through the center of the source parallel to the incident light beam by an amount numerically equal to the specific angular momentum a of the lens irrespective of the impact parameter and the mass of the lens.

Second, it is found that the dependence of the photon propagation time on the orientation of its orbital angular momentum relative to the rotation axis leads to a relative delay of the rays focused by the rotating massive body. The action of the gravitational lens leads to the appearance of multiple images of an isolated radiation source formed by rays that travel along different optical paths. In the case when the radiation source, the nonrotating point mass that plays the part of the lens, and the observer are situated on a single straight line, the resulting images are simultaneous, i.e., the signals propagate from a given point of the source along the different optical paths corresponding to the different images in the same time. In the case of an extended gravitational lens with spherically symmetric density distribution and when the observer is on the straight line joining the radiation source and the center of the lens, all the rays arriving at the observer arrive simultaneously (this assertion can be verified by using, for example, Ref. 17, Vol. 2, p. 324).

Rotation of the gravitational lens leads to nonsimultaneity of the resulting images even in the simplest case when the source of the radiation, the lens, and the observer are on the same straight line. The relative delay between rays arriving at the same point of observation along different optical paths is maximal in the equatorial plane of the focusing body. The condition that the radiation source, the lens, and the observer are on one line has the form[8]

$$\frac{d}{b}+\frac{d}{f}=\frac{4}{d}-\frac{4a}{d^2}\frac{\rho_\perp}{|\rho_\perp|}+\frac{15\pi-32}{4d^2}, \tag{9.1}$$

where b is the distance from the lens to the point of emission, and f is the distance to the point of observation (Fig. 22). It follows from this relation that rays emanating from the same point of the source with positive and negative impact parameters can arrive at the same point of observation only if they satisfy the condition

$$d_- = d_+ + a. \tag{9.2}$$

As a result, there arises a relative delay in time associated with the difference of the optical paths between rays arriving at the same point of observation; it is given by

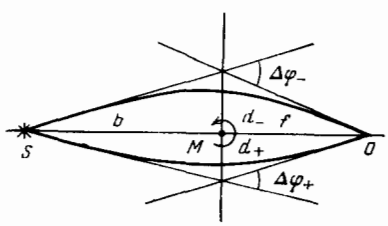

FIG. 22. Deviation of rays traveling from a point of the source S in the equatorial plane of the rotating body M to the point of observation 0; d_+, d_- and $\Delta\varphi_+$, $\Delta\varphi_-$ are the distances of closest approach and the deflection angles of rays possessing positive and negative impact parameters.

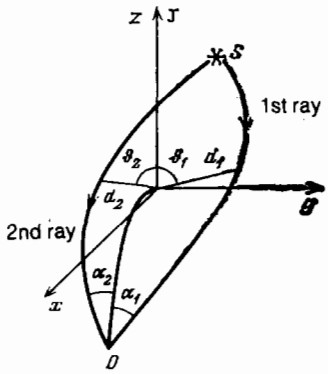

FIG. 23. Paths of rays in a Kerr gravitational lens in the general case; S is the radiation source, O is the observer, and J is the angular momentum of the lens.

$$\Delta t = t_- - t_+ = \frac{8a}{d} GMc^{-3}. \tag{9.3}$$

The relative delay depends on the type of focusing object and the mutual disposition of the source, lens, and observer. It lies in the range

$$\Delta t = 2\cdot10^{-6}\ \text{sec}\cdot\left(\frac{M}{5M_\odot}\right)\left(\frac{a}{1}\right)\left(\frac{100}{d}\right)$$
$$= 200\ \text{sec}\cdot\left(\frac{M}{5\cdot10^8M_\odot}\right)\left(\frac{a}{1}\right)\left(\frac{100}{d}\right). \tag{9.4}$$

In the general case, when the radiation source is not in the equatorial plane of the lens, the expression for the relative delay has a more complicated form[20]:

$$\Delta T = f\left(1+\frac{f}{b}\right)\left\{\frac{\alpha_2^2-\alpha_1^2}{2}+\right.$$
$$+\alpha_1\alpha_2\left[4\rho\tan\vartheta_d\cos\eta_d\right.$$
$$\left.\left.+\frac{|\alpha_2-\alpha_1|}{4}\left(1+\frac{f}{b}\right)\left(\frac{15\pi}{8}-1\right)\right]-4\ln\frac{|\alpha_1|}{\alpha_2}\right\}. \tag{9.5}$$

The path of the rays is shown in this case in Fig. 23, where α_1 and α_2 are the intervals of the angular variable

$$\alpha_{1,2}=\frac{d_{1,2}}{f}\left(1+\frac{1}{d_{1,2}}\pm\frac{ae}{d_{1,2}}\right),$$

joining the images to the lens and forming with each other the angle

$$\rho=\frac{a|\cos\vartheta_d|}{f}\left(\frac{1}{\alpha_1}+\frac{1}{\alpha_2}\right).$$

As ϑ_d, one can take ϑ_1 or ϑ_2, the accuracy of the calculation being unaffected.[20]

Rotation of the lens can lead to curious consequences in the case when the lens is a rotating black hole situated on the line of sight between the observer and a source of radiation that has dimensions greater than the angular dimensions of the lens. In this case, as we have already said, the black hole must be seen literally as a black hole in the image of the source, surrounded by an asymmetric luminous halo formed by photons deflected by the hole through the angles (7.13). As a result of the asymmetry of the scattering, there must be a relative time delay of the propagation of the photons forming the boundary of the image of the hole. The relative delay of the photons propagating in the equatorial plane with maximal and minimal impact parameters is given by[8]

$$\Delta t \approx 3 \mid \Delta\varphi \mid GMc^{-3}. \quad (9.6)$$

In the case of a variable source of radiation, this may have the consequence that if the brightness of the source changes the brightness of the boundary curve will vary nonuniformly, and a "hare" will run round it from the point corresponding to the minimal value of the impact parameter ρ_1, with velocity $v_h \approx (c/6)R_S/R_H$ (for an extremal black hole), where R_H is the distance from the observer to the black hole, and R_S is the distance from the observer to the radiation source.

The relative delay of signals focused by a rotating gravitational lens in the case when the lens is a massive black hole is characterized by a quantity that is perfectly measurable, though it is at present difficult to give a specific example of the realization of such a situation. However, there have long been reports of the observation of extremely rapid variability in time of the radiation intensity from cosmic objects. In particular, the quasar 1525 + 227 exhibits a variation of its radiation intensity with a characteristic time $\tau \approx 200$ sec.[75] For an object of the scale of a quasar, this time interval is so short that it is difficult to explain it by processes taking place in the quasar itself. One could assume that the rapid variability in the radiation intensity could in some cases be due to the effect of a rotating gravitational lens situated between the quasar and the observer. In principle, such a possibility does not seem unjustified.

I should like to thank L. P. Grishchuk, A. Z. Dolginov, Ya. B. Zel'dovich, A. D. Kaminker, N. N. Kostyukovich, Yu. É. Lyubarskiĭ, I. D. Novikov, and Ya. A. Smorodinskiĭ for helpful discussions and critical comments.

[1)]By this we mean test bodies without intrinsic rotation.

[2)]The fact of the existence of an additional constant of the motion has an analogy in mechanics, for example, there is the conservation of L_z and P_z for motion in the field of an infinite homogeneous cylinder (Ref. 17, Vol. 1, p. 33).

[3)]By April 1984, five gravitational lenses were known (Sky and Telescope, April 1984).

[1]A. F. Bogorodskiĭ, Uravneniya polya Éĭnshteĭna i ikh primenenie v astronomii (Einstein's Field Equations and their Applications in Astronomy), Izd. Kiev Univ., Kiev, 1962.
[2]S. Weinberg, Gravitation and Cosmology, Wiley, New York, 1972 (Russ. Transl., Mir, M., 1975).
[3]S. Gupta, in: Problemy statisticheskoĭ i kvantovoĭ fiziki (Problems of Statistical and Quantum Physics; Russ. Transl.), UDN, M., 1980, p. 82.
[4]A. G. Doroshkevich, Astron. Zh. **43**, 105 (1966).
[5]I. G. Dymnikova, in: Tezisy Vsesoyuznoĭ gravitatoionnoĭ konferentsii (Abstracts of All-Union Gravitational Conference), Minsk, 1976, p. 126.
[6]I. G. Dymnikova, Yad. Fiz. **31**, 679 (1980) [Sov. J. Nucl. Phys. **31**, 353 (1980)].
[7]I. G. Dymnikova, Preprint No. 795 [in Russian], A. F. Ioffe Physicotechnical Institute, Leningrad, 1982.
[8]I. G. Dymnikova, Zh. Eksp. Teor. Fiz. **86**, 385 (1984) [Sov. Phys. JETP **59**, 223 (1984)].
[9]I. T. Zhuk and K. A. Piragas, Izv. Vyssh. Uchebn. Zaved. Fiz. **4**, 77 (1982) [Sov. Phys. J. **25**, 358 (1982)].
[10]Ya. D. Zel'dovich and I. D. Novikov, Teoriya tyagoteniya i évolyutsiya zvezd (The Theory of Gravitation and the Evolution of Stars), Nauka, M., 1971.
[11]Ya. B. Zel'dovich, Pis'ma Zh. Eksp. Teor. Fiz. **14**, 270 (1971) [JETP Lett. **14**, 180 (1971)].
[12]S. V. Izmaĭlov and E. S. Levin, Izv. Vyssh. Uchebn. Zaved Fiz. **5**, 17 (1979); **8**, 3 (1980) [Sov. Phys. J. **22**, 472 (1979); **23**, 645 (1981)].
[13]N. N. Kostyukovich and V. V. Mityankov, Acta, Phys. Pol. **B10**, 279 (1979).
[14]O. P. Krivenko and K. A. Piragas, Preprint 73-38R [in Russian], Institute of Theoretical Physics, Kiev (1973).
[15]A. P. Lightman, R. A. Syunyaev *et al.*, Comments on Astrophysics 7(5), 151 (1978) [Russ. Transl. Usp. Fiz. Nauk **126**, 515 (1978)].
[16]A. P. Lightman, W. H. Press, R. Price, and S. Teukolsky, Problem book in relativity and gravitation, Princeton University Press, 1975 [Russ. Transl., Mir, M., 1979].
[17]L. D. Landau and E. M. Lifshitz, Teoreticheskaya Fizika, T. 1, Mekhanika, T. 2, Teoriya polya, Nauka, M., 1971, 1973 [Engl. Transl.: Mechanics, 3rd Ed., Pergamon Press, Oxford, 1976; The Classical Theory of Fields, 4th ed., Pergamon Press, Oxford, 1975].
[18]C. W. Misner, K. S. Thorne, and J. A. Wheeler, *Gravitation*, W. H. Freeman, San Francisco, 1973 (Russ. Transl., Mir, M., 1977).
[19]N. V. Mitskevich, in: Problemy teorii gravitatsii i élementarnykh chastits (Problems of the Theory of Gravitation and Elementary Particles), No. 7, Atomizdat, M., 1976, p. 15; N. V. Mitskevich and P. Garcia, Dokl. Akad. Nauk SSSR, **192**, 1263 (1970) [Sov. Phys. Dokl. **15**, 383 (1970)].
[20]N. V. Mitskevich and A. V. Ul'din, Effekt gravitatsionnoĭ linzy v pole Kerra (Gravitational Lens Effect in the Kerr Field), Manuscript Deposited at VINITI, No. 2654-83, USSR Academy of Sciences (1983); A. V. Ul'din and A. V. Vaĭvod, Kvazigiperbolicheskie traektorii lucha sveta v pole Kerra (Quasihyperbolic Trajectories of a Light Ray in the Kerr Field), Manuscript Deposited at VINITI, No. 847-83, USSR Academy of Sciences (1983).
[21]A. A. Minakov, Izv. Vyssh. Uchebn. Zaved. Radiofiz. **3**, 388 (1981).
[22]V. F. Mukhanov, Usp. Fiz. Nauk **133**, 729 (1981) [Sov. Phys. Usp. **24**, 331 (1981)].
[23]I. D. Novikov and A. G. Polnarev, Priroda (Moscow) **7**, 12 (1980).
[24]J. R. Oppenheimer and H. Snyder, a) in: Al'bert Eĭnshteĭn i teoriya gravitatsii (Albert Einstein and the Theory of Gravitation; Russ. Transl., Mir, M., 1979, p. 353; b) Phys. Rev. **56**, 455 (1939).
[25]A. G. Polnarjev and V. I. Turchaninov, Acta Phys. Pol. **29**, 81 (1979).
[26]M. J. Rees, R. Ruffini, and J. A. Wheeler, *Black Holes, Gravitational Waves and Cosmology*, Gordon and Breach, New York (1976) [Russ. Transl., Mir, M., 1977].
[27]G. V. Sktroskiĭ, Dokl. Akad. Nauk SSSR **114**, 73 (1957) [Sov. Phys. Dokl. **2**, 226 (1958)].
[28]A. A. Starobinskiĭ, Zh. Eksp. Teor. Fiz. **64**, 48 (1973) [Sov. Phys. JETP **37**, 28 (1973)]; A. A. Starobinskiĭ and S. M. Churilov, Zh. Eksp. Teor. Fiz. **65**, 3 (1973) [Sov. Phys. JETP **38**, 1 (1974)].
[29]K. S. Thorne, *The search for black holes* [Russ. Transl., Usp. Fiz. Nauk **118**, 453 (1976)].
[30]V. P. Frolov, Usp. Fiz. Nauk **118**, 473 (1976) [Sov. Phys. Usp. **19**, 244 (1976)].
[31]S. Hawking, in the book of Ref. 24a, p. 479.
[32]D. G. Yakovlev, Zh. Eksp. Teor. Fiz. **68**, 369 (1975) [Sov. Phys. JETP **41**, 179 (1975)].
[33]J. M. Bardeen, Nature **226**, 64 (1970).
[34]J. M. Bardeen, W. H. Press, and S. A. Teukolsky, Astrophys. J. **178**, 347 (1972).
[35]J. M. Bardeen, in: Black Holes (eds. C. DeWitt and B. S. DeWitt), Gordon and Breach, New York, 1973.
[36]J. M. Bardeen, in: Gravitational Radiation and Gravitational Collapse: IAU Symposium 64 (ed. C. DeWitt-Morette), D. Reidel, Dordrecht, Holland, 1974.
[37]J. M. Bardeen and J. A. Petterson, Astrophys. J. **195**, L65 (1975).
[38]J. Bićak and Z. Stuchlik, Bull. Astrophys. Inst. Czech. **27**, 129 (1976).
[39]J. Bićak and Z. Stuchlik, Mon. Not. R. Astron. Soc. **175**, 381 (1976).
[40]R. D. Blandford and K. S. Thorne, in: General Relativity: An Einstein Centenary Survey (eds. S. Hawking and W. Israel), University Press, Cambridge (1979) [Russ. Transl., Mir, M., 1983].
[41]S. K. Bose and M. Y. Wang, J. Math. Phys. (N. Y.) **15**, 957 (1974).
[42]L. H. Boyer and R. W. Lindquist, J. Math. Phys. (N. Y.) **8**, 265 (1967).
[43]R. H. Boyer and T. G. Price, Proc. Cambridge Philos. Soc. **61**, 531 (1965).
[44]M. Calvani and F. de Felice, Gen. Rel. Grav. **9**, 889 (1978).
[45]M. Calvani, F. de Felice, and Z. Nobili, J. Phys. A **13**, 3213 (1980).
[46]M. Calvani, F. de Felice, R. Fabbri, and R. Turolla, Nuovo Cimento **B67**, 1 (1982).
[47]M. Calvani and Z. Suchlik, Nuovo Cimento **B70**, 128 (1982).
[48]M. Calvani and R. J. Turolla, J. Phys. A **14**, 1931 (1981).
[49]B. Carter, Phys. Rev. **141**, 1242 (1966).
[50]B. Carter, Phys. Rev. **174**, 1559 (1968).
[51]S. Chandrasekhar, In the book of Ref. 40 (p. 370 of Russ. Transl.).
[52]D. Christodoulou, Phys. Rev. Lett. **25**, 1596 (1970).
[53]D. Christodoulou and R. Ruffini, Phys. Rev. D **4**, 3552 (1971).

[54]J. Cohn, Am. J. Phys. **45**, 239 (1977).
[55]P. A. Collins, R. Delbourgo, and R. M. Williams, J. Phys. A **6**, 161 (1973).
[56]C. D. Collinson and P. N. Smith, Commun. Math. Phys. **56**, 277 (1977).
[57]C. T. Cunningham and J. M. Bardeen, Astrophys. J. **183**, 237 (1973).
[58]C. T. Cunningham, Astrophys. J. **202**, 788 (1975); **208**, 534 (1976).
[59]N. Dadhich and P. P. Kale, J. Math. Phys. (N. Y.) **18**, 1727 (1977); Pramana **9**, 71 (1977).
[60]F. de Felice, Nuovo Cimento **B57**, 351 (1968).
[61]F. de Felice and M. Calvani, Nuovo Cimento **B10**, 447 (1972).
[62]F. de Felice, Phys. Lett. **A69**, 307 (1969).
[63]F. de Felice, Phys. Rev. D **19**, 451 (1979).
[64]F. de Felice, J. Phys. A **13**, 1701 (1980).
[65]F. de Felice, L. Nobili, and M. Calvani, J. Phys. A **13**, 2401, 3635 (1980).
[66]B. B. Godfrey, Phys. Rev. D **1**, 2721 (1970).
[67]H. Goldstein, Z. Phys. **271**, 275 (1974).
[68]L. Hughston, R. Penrose, P. Sommers, and M. Walker, Commun. Math. Phys. **27**, 303 (1972).
[69]L. Hughston and P. Sommers, Commun. Math. Phys. **33**, 129 (1973).
[70]R. P. Kerr, Phys. Rev. Lett. **11**, 237 (1963).
[71]M. M. Kumar, Lett. Nuovo Cimento **28**, 269 (1980).
[72]J. K. Lawrence, Astrophys. J. **239**, 305 (1980).
[73]J. Lense and H. Thirring, Phys. Z. **19**, 156 (1918).
[74]B. Mashhoon, Astrophys. J. **216**, 591 (1977).
[75]T. Matilsky, C. Shraeder, and H. Tananbaum, Astrophys. J. **258**, LI (1982).
[76]C. W. Misner, Bull. Am. Phys. Soc. **17**, 472 (1972).
[77]I. D. Novikov and K. S. Thorne, In the book of Ref. 35, p. 343.
[78]R. Penrose, Riv. Nuovo Cimento **1**, Spec. Issue, 252 (1969).
[79]J. Plebanski, Phys. Rev. **118**, 1396 (1960).
[80]A. R. Prasanna, Riv. Nuovo Cimento **3**, 11 (1980).
[81]W. H. Press and S. A. Teukolsky, Nature **238**, 211 (1972).
[82]W. H. Press and S. A. Teukolsky, Astrophys. J. **141**, 443 (1974).
[83]M. J. Rees, Proc. R. Soc. London Ser. A: **368**, 27 (1979).
[84]R. Ruffini and J. A. Wheeler, "Relativistic cosmology and space platforms," in: Proc. of Conference on Space Physics, Europ. Space Organ., Paris, 1971.
[85]N. A. Sharp, Gen. Rel. Grav. **10**, 659 (1979).
[86]N. A. Sharp, J. Comput. Phys. **41**, 295 (1981).
[87]M. Sikora, Acta Astron. Pol. **29**, 87 (1979).
[88]J. M. Stewart and M. Walker, Black Holes: The Outside Story, Springer-Verlag, Berlin (1973).
[89]Z. Stuchlik, Bull. Astron. Inst. Czech. **31**, 129 (1980); **32**, 40 (1981).
[90]S. A. Teukolsky, Phys. Rev. Lett. **29**, 1114 (1972).
[91]M. Walker and R. Penrose, Commun. Math. Phys. **18**, 265 (1970).
[92]D. Walsh, R. F. Carswell, and R. J. Weymann, Nature **279**, 381 (1979).
[93]R. J. Weymann, D. Latham, J. R. P. Angel *et al.*, Nature **285**, 641 (1980).
[94]D. W. Weedman, R. J. Weymann, R. F. Green, and T. M. Heckman, Astrophys. J. **255**, L5 (1982).
[95]D. Wilkins,Phys. Rev. D **5**, 814 (1972).
[96]M. Yohnston and R. Ruffini, Phys. Rev. D **10**, 2324 (1974).
[97]P. J. Young, Phys. Rev. D **14**, 3281 (1976).
[98]V. B. Braginskiĭ and A. G. Polnarev, Pis'ma Zh. Eksp. Teor. Fiz. **31**, 444 (1980) [JETP Lett. **31**, 415 (1980)].
[99]V. L. Ginzburg, Dokl. Akad. Nauk SSSR **156**, 43 (1964) [Sov. Phys. Dokl. **9**, 329 (1964)].
[100]A. G. Doroshkevich, Ya. B. Zel'dovich, and I. D. Novikov, Zh. Eksp. Teor. Fiz. **49**, 170 (1965) [Sov. Phys. JETP **22**, 122 (1966)].
[101]Ya. B. Zel'dovich, Pis'ma Zh. Eksp. Teor. **1**, 40 (1965) [JETP Lett. **1**, 95 (1965)].
[102]Ya. B. Zel'dovich, Pis'ma Zh. Eksp. Teor. Fiz. **14**, 270 (1971) [JETP Lett. **14**, 180 (1971)].
[103]Ya. B. Zel'dovich, Zh. Eksp. Teor. Fiz. **62**, 2076 (1972) [Sov. Phys. JETP **35**, 1085 (1972)].
[104]Ya. B. Zel'dovich and I. D. Novikov, Astron. Zh. **43**, 758 (1966) [Sov. Astron. **10**, 602 (1967)].
[105]Ya. B. Zel'dovich and M. A. Podurets, Astron. Zh. **42**, 963 (1965) [Sov. Astron. **9**, 742 (1965)].
[106]N. S. Kardashev, I. D. Novikov, A. G. Polnarev, and B. E. Shtern, Astron. Zh. **60**, 209 (1983) [Sov. Astron. **27**, 119 (1983)].
[107]A. G. Polnarev and M. Yu. Khlopov, Usp. Fiz. Nauk **145**, 369 (1985) [Sov. Phys. Usp. **28**, 213 (1985)].
[108]R. D. Blandford and R. L. Znajek, Mon. Not. R. Astron. Soc. **179**, 433 (1977).
[109]R. D. Blandford, in: Proc. of AIP Conference: The Galactic Center (eds. G. R. Reigler and R. D. Blandford), Calif. Inst. Techn. New York (1982), p. 177 (Russ. Transl., Mir, M., 1984, p. 224).
[110]V. B. Braginsky, C. M. Caves, and K. S. Thorne, Phys. Rev. D **15**, 2047 (1977).
[111]V. B. Braginsky, A. G. Polnarjev, and K. S. Thorne, Phys. Rev. Lett. **53**, 863 (1984).
[112]S. Chandrasekhar, The Mathematical Theory of Black Holes, Clarendon Press, Oxford (1983).
[113]L. H. Ford, J. Phys. A **15**, 825 (1982).
[114]M. Kafatos, Astrophys. J. **236**, 99 (1980).
[115]A. Kovetz, Lett. Nuovo Cimento **12**, 39 (1975); A. Kovetz and Z. Piran, Lett. Nuovo Cimento **12**, 560 (1975).
[116]P. C. Laplace, Allgemeine geographische Ephemeriden, verfassed von einer Gesellschaft Gelehrter. Bd I, Weimar: F. X. von Zach 1799; translated in: S. W. Hawking and G. F. R. Ellis, The Large Scale Structure of Space-Time, CUP (1973).
[117]D. Leiter and M. Kafatos, Astrophys. J. **226**, 32 (1978); **229**, 46 (1979).
[118]T. Piran, J. Shaham, and J. Katz, Astrophys. J. **196**, L107 (1975); T. Piran and J. Shaham, Phys. Rev. D **16**, 1615 (1977).
[119]M. J. Rees, Contemp. Phys. **21**, 99 (1980).
[120]M. J. Rees, In book of Ref. 109 [p. 166 Engl., p. 209 Russ.].
[121]C. M. Will, Astrophys. J. **196**, 41 (1975).
[122]R. H. Price and K. S. Thorne, Caltech Preprint GRP-038, 1985; R. L. Znajek, Mon. Not. R. Astron. Soc. **185**, 833 (1978); T. Damour,Phys. Rev. D **18**, 3598 (1978); K. S. Thorne and D. A. Macdonald, Mon. Not. R. Astron. Soc. **198**, 339 (1982); D. A. Macdonald and K. S. Thorne, Mon. Not. R. Astron. Soc. **198**, 345 (1982).
[123]F. K. Manasse, J. Math. Phys. (N. Y.) **4**, 746 (1963); M. Demianski and L. P. Grishchuk, Gen. Rel. Grav. **5**, 673 (1974); P. D'Eath, Phys. Rev. D **12**, 2183 (1975); K. S. Thorne and J. B. Hartle, Phys. Rev. D **31**, 1815 (1985); T. Damour, in: Gravitational Radiation (eds. N. Deruelle and T. Piran), North-Holland, Amsterdam, 1983, p. 59; L. P. Grishchuk and S. M. Kopejkin, in: Proc. of Symposium IAU No. 114, Leningrad (1985) (in press).

Translated by Julian B. Barbour